Research and Test Department

Chicago Technical Center

ASSOCIATION
OF AMERICAN
RAILROADS

Association of American Railroads
Research and Test Department

LABORATORY FATIGUE TESTING OF WELDED AND BOLTED ALUMINUM CONNECTIONS FOR FREIGHT CAR DESIGN

Report No. R-839

W. H. Walker
Department of Civil Engineering
University of Illinois at Urbana-Champaign
F. V. Lawrence, Jr.
Department of Civil Engineering
University of Illinois at Urbana-Champaign
V. Sharma
Research and Test Department
Association of American Railroads

June, 1993

AAR Technical Center
Chicago, Illinois

DISCLAIMER

This report is disseminated by the Association of American Railroads (AAR) and the Federal Railroad Administration (FRA) for informational purposes only and is given to, and accepted by, the recipient at its sole risk. The AAR and FRA make no representations or warranties, either expressed or implied, with respect to the report or its contents. The AAR and FRA assume no liability to anyone for special, collateral, exemplary, indirect, incidental, consequential or any other kind of damage resulting from the use or application of this report or its contents. Any attempt to apply the information contained in this report is done at the recipient's own risk.

1. REPORT NO. R-839	**2. REPORT DATE** June, 1993	**3. PERIOD COVERED** January 1990 to September 1992
4. TITLE AND SUBTITLE Laboratory Fatigue Testing of Selected Welded and Bolted Aluminum Connections for Freight Car Design		
5. AUTHOR (S) W.H.Walker and F.V.Lawrence,Jr. Department of Civil Engineering University of Illinois at Urbana-Champaign	V. Sharma Research and Test Department Association of American Railroads	
6. PERFORMING ORGANIZATION NAME AND ADDRESS Department of Civil Engineering University of Illinois at Urbana-Champaign 1116 Newmark Laboratory MC-205 205 North Mathews Avenue Urbana, IL 61801-2397	**7. TYPE OF REPORT** Research **8. CONTRACT OR GRANT NO.** DTFR 53-86-C-00011	
9. SPONSORING AGENCY NAME AND ADDRESS Federal Railroad Administration 400 7th Street, S.W. Washington, D.C. 20590	**10. NO. OF PAGES** 102 **11. NO. OF REFERENCES** 5	
12. SUPPLEMENTARY NOTES		

13. ABSTRACT

This report describes the tests conducted to determine the fatigue properties of joints and construction details in aluminum-bodied freight cars. The tests were conducted at the Department of Civil Engineering of the University of Illinois at Urbana-Champaign. The funding for this test program was provided by the Association of American Railroads and the Federal Railroad Administration. Technical guidance was provided by the Freight Car Structures Fatigue Task Force.

With the growing use of aluminum in lightweight freight cars, the importance of designing cars against premature failure from fatigue can hardly be overstated. Fatigue failures can occur at inadequately designed construction details.

Eleven joint and details were selected for this test program, based on a survey of the needs of the industry. These joints and details were built using 5083 and 5086 aluminum alloys for sheets and 6061 series for extrusions. These are the commonly used aluminum alloys in freight car construction. The test specimen were fabricated by the freight car builders to ensure that the specimens reflected the fabricating and welding techniques used in actual construction.

The data obtained through this test program will augment that available in the AAR Mechanical Division's "Specification for Design and Construction of Freight Cars"(M-1001)

14. SUBJECT TERMS Freight car, Aluminum, Fatigue properties, S-N diagram, Modified Goodman diagram, Fatigue testing, Aluminum connections and details	**15. AVAILABILITY STATEMENT** Document Distribution Center Association of American Railroads Technical Center 3140 South Federal Street Chicago, Illinois 60616

ASSOCIATION OF AMERICAN RAILROADS | RESEARCH AND TEST DEPARTMENT

REQUEST for FEEDBACK

Report No: ____________ Report Title: ______________________________________

YES	NO	
❑	❑	Did you find the report useful for your particular needs? If so, how
❑	❑	Did you find the research to be of high quality?
❑	❑	Were the results of the research communicated effectively by this report?
❑	❑	Do you think this report will be valuable to workers in the technical area represented by the subject area of the research?
❑	❑	Are there one or more areas of the report which need strengthening? Which areas?
❑	❑	If you do not already, would you be interested in receiving Report Briefs and Research Highlights covering AAR research?

Please furnish in the space below any comments you may have concerning the report. We are particularly interested in further elaboration of the above questions.

COMMENTS

NAME: ______________________________

TITLE: ______________________________

COMPANY: ______________________________

ADDRESS: ______________________________

____

Thank you for your cooperation. Please forward your comments to:
A. J. Reinschmidt, Assistant Vice President, Chicago Technical Center
3140 South Federal Street, Chicago, Illinois, 60616

EXECUTIVE SUMMARY

With the growing use of aluminum in lightweight cars, the importance of designing cars against premature failure from fatigue can hardly be overstated. Fatigue failures can occur at inadequately designed construction details.

Tests designed to determine the fatigue properties of joints and construction details in aluminum-bodied freight cars and the stresses found near welds in aluminum components were conducted at the University of Illinois, Urbana. Funding for this work was provided by the Association of American Railroads and the Federal Railroad Administration.

The data obtained through this research will augment that available in the AAR Mechanical Division's Specification for Design and Construction of Freight Cars (M-1001).

Full size test specimens were built using 5083 and 5086 aluminum alloys for sheets and 6061 alloys for extrusions. These alloys are used in aluminum freight car construction.

Specimen fabrication followed typical car building practices. Ordinary welding practices were followed with no intent to create defects or exceptional welds, except for one series of tests on partial penetration butt welds. All specimens were fabricated by car builders and shipped to the Newmark Laboratory of the University of Illinois at Urbana-Champaign for testing.

Eleven joints and details were selected based on a survey

of the needs of the industry. They permit these parts and connections to be analyzed :

- A steel-plate-to-aluminum connection using Huck bolts in single-shear and double-shear lap joints - for example, a shear-plate-to-carbody connection.
- The connection of a side-sill extrusion to a side-sheet using either a butt weld or a combination fillet weld and butt weld.
- The connection of a diagonal brace to the top chord on open-top high-side gondolas and hopper cars.
- Fabricated body bolster details. This beam specimen is 12 feet long, 13 1/4 inches in depth over-all, and utilizes 3/8-inch to 5/8-inch aluminum plates.
- Cover-plate termination details for large structural members such as center sills.
- The use of intermittent welds instead of full welds for lap joints.
- The use of slot welds in members such as the sole plates of body bolsters, and in draft sills.

Essentially, for each type of connection or structural element for which data were required, a test specimen configuration was designed. At least six specimens were subjected to constant amplitude cyclic fatigue tests in a servo-controlled test machine until crack initiation, substantial propagation and failure resulted. Stress levels were selected to provide data on fatigue life in the 100,000 cycle to 2,000,000 cycle range.

Also, the concentrations of stress near welds and at weld terminations near Huck bolts were measured using a device called 'SPATE', Stress Pattern Analysis by the Thermographic Emissions. SPATE is a computer-controlled instrument for making noncontact measurements of dynamic stresses in components and structures. The technique is based on measuring the thermoelastic effect, or Kelvin effect. The AAR acquired a SPATE unit in 1989 and the associated hardware needed to examine structures with large deformations in 1990.

The commentary and discussion, presented for each test series, generally indicates that the behaviour of the connections was within expectations for the detail geometries tested.

The following general conclusions and accompanying recommendations should be noted :

- Single lap connections are sensitive to bending stresses introduced at the critical section. Car Designers should account for this bending in their analysis.
- The bolted beam cover plate termination is an effective detail. Additional future tests should be considered to optimize the number and location of the bolts.
- The aluminum box section with interrupted webs

behaves like its steel counterpart.

- The diagonal brace connection, which is a pad to tube connection, showed a marked amount of pad flexing.

TABLE OF CONTENTS

LIST OF TABLES

LIST OF EXHIBITS

LIST OF SYMBOLS

A0	Log intercept of the regression line for the S-N diagram.
A1	Slope of the regression line for the S-N diagram.
C	Life coefficient as defined in $N = C/S^m$
m	fatigue life exponent as defined in $N = C/S^m$
N	Fatigue life in cycles (or 1000's of cycles)
R	Stress ratio = (minimum stress range)/(maximum stress range)
S	Stress range in ksi
ρ	Correlation coefficient of the regression line for the S-N diagram.

ACKNOWLEDGEMENTS

This study was sponsored by the Federal Railroad Administration under the Association of American Railroad's Vehicle Track System Program, Fatigue Task Force. Messrs. Gordon Stevens and Donald Gray served as the FRA Task Monitors. The project was monitored by John Punwani and Vinaya Sharma at the AAR. The research was conducted in the Department of Civil Engineering under the supervision of Dr. Walker. Project staff included Patrick Cassity, graduate research assistant. Harold Dalrymple, Research Engineer, coordinated testing in the laboratory and was responsible for the operation of the hydraulic testing apparatus. The assistance of Carroll Swan, shop supervisor, and his staff in fabrication of test fixtures and other support was greatly appreciated. Mr. William Sneed of AAR operated the SPATE unit.

Thanks are due to the firms which supplied materials and fabricated the specimens tested in this project. The participating firms were National Steel Car Limited of Hamilton, Ontario, Thrall Car Manufacturing Company of Chicago Heights, Illinois, Ortner Freight Car Division of Trinity Industries, Inc., of Mt. Orab, Ohio, ALCAN International, Canada and Bethlehem Steel Freight Car Division.

1.0 GENERAL

1.1 INTRODUCTION

The current design methodology which has been developed by the Association of American Railroads for freight cars is described in the Manual of Standards and Recommended Practices, Section C, Part II, which includes specifications for design, fabrication and construction of freight cars. The methods of this document are based on the use of linear cumulative damage (Miner's Rule) in conjunction with modified Goodman diagrams. The standard is based upon laboratory fatigue testing, under constant amplitude, of both welded and bolted aluminum as well as steel details, used in freight car construction. To extend the usefulness of this design procedure the actual load histories experienced by freight cars during service were corrected for a number of car types including the service history of fully-laden, 70-ton box cars and 100-ton high-side coal gondolas, and five unit spine cars. Such information can now be used in conjunction with existing design methodology to take into account the actual service history experienced by freight cars to estimate the fatigue life.

1.2 OBJECT AND SCOPE

The intent of this study, Material Fatigue Properties Data Development, as prepared by the Vehicle Track Systems (VTS) Committee of the Association of American Railroads was to continue the laboratory fatigue testing of selected details in details in aluminum with the intent of filling gaps in the available fatigue data for weldments and selected bolted connections, and to investigate the fatigue behavior of feasible alternative materials not currently included in freight car design documentation.

The matrix of tests conducted is tabulated below:

Table 1.1 Matrix of Tests Conducted

Detail	Description	Stress Ratio, R	Number of Tests
A	Single Huck-Bolted Lap Splice	0, 0.5	32
B	Double Huck-bolted Splice	0, 0.5	27
C	Side Sheet to Sill Connection with Butt Weld	0	6
D	Side Sheet to Sill Connection with Butt and Fillet Weld	0	7
E	Partial Penetration Butt Weld	0	8
F	Brace to Top Chord Connection	0	7
G	Box (Bolster) Beam with Interrupted Web	0	6
H	I-Beam with Cover Plates, Huck Bolted Termination and Longitudinal Welds	0	6
I	Welded Single Lap Splice	0	8
J	Slot-Welded Lap Splice	0	6
K	Slot Welded Lap Splice with Side Fillet Welds	0	6
			119 (Total)

For Details A and B, it was not possible to run reliable tests for R = -1 (under full reversal) because of the low critical buckling capacity associated with the relatively thin aluminum plates used in these details.

1.3 MATERIALS TESTED

The primary focus of the test program was to evaluate details fabricated in 5083-H321 aluminum plate. The exception was the use of 6061-T6 alloy for the aluminum tube brace in Series F. Series A and B also used steel plate elements for which A441 steel was selected. The bolts used in Series A, B, and H were commercial 5/8" diameter Huck bolts.

1.4 ORGANIZATION OF REPORT

The discussion of the results is grouped by approximate function of the tested details and elements. Section 2 is devoted to welded splice and connection details. Section 3 presents the results of the bolted tension connections, single and double shear type behavior. Section 4 is concerned with the flexural tests. Section 5 describes the SPATE demonstration. The results of the study are summarized in brief, regression results for S-N diagrams are summarized, and recommendations for future studies are presented in Section 6.

1.5 SUMMARY OF RESULTS

This section is intended to highlight the results of the sented. Detailed discussion and tabulated as well as plotted results are presented in Sections 2, 3 and 4.

The lack of axial symmetry in the tension splices tested produced significant factors in behavior. For the lap splices, transverse welded and slot welded, the effects of flexure due to eccentricity of axial loading were evident. Substantial out-of-plane motions were observed and cracking initiated at points of stress concentration in the zone of high flexure.

The behavior of the bolted single and double lap splices reflected a specimen geometry in which the net section controlled. No evidence of distress in the bolts was observed. For the single lap splice the influence of eccentricity of axial loading was evident. For the double lap splice the ratio of net section to gross section in the grips was not sufficiently large to assure that failure always initiated in the net section rather than at the testing machine grips.

The simulated brace-to-top chord connection showed the flexibility of the pads used in the connection detail, but failure always initiated in the fillet weld connecting the tube tension member to the first pad element. At no time did cracking penetrate into the plates representing the main chord member.

From the box beam flexural fatigue tests, it is clear that any interruptions introduced in the web decrease the fatigue life of the beam. This configuration represents the freight car body bolster/sill geometry. This result is consistent with that observed for similar steel box beams (see Ref. 1).

The use of partial length cover plates is the least desirable detail for fatigue performance in beam elements. However, the use of bolted cover plate terminations is shown to be highly favorable. In the present studies, the use of a four-bolt termination moved the point of failure to the simple net section of the outer line of bolts. In fact, in one test in the series, a failure occurred at midspan rather than at the coverplate termination point.

1.6 RECOMMENDATIONS

The basic task of the program was to provide data to augment the fatigue data base for design and analysis. In the course of this effort the following recommendations are seen:

1. The tests of single and double Huck-bolted tension splices show the need for revised specimen geometry, particularly to permit full reversal tests. In addition, if more detailed studies of bolt behavior are desired, then tests with suitable variation in bolt parameters should be undertaken.

2. The single lap connections, both welded and bolted, are sensitive to the flexural stress induced at the critical section. The flexural behavior is greatly influenced by the relative flexural stiffness of the connected elements. The relatively slender specimens tested in this study should be

evaluated for their suitability in representing "single plane shear" in actual connections between car elements.

3. The bolted beam coverplate termination was found to be an effective detail to improve coverplate behavior. The optimum number of bolts and their arrangement could be a target for future study.

4. The aluminum box with interrupted webs, representing the bolster beam, exhibits the same form of damage as it's counterpart in steel. It is important that the geometry of this element be typical of the actual bolster detail.

5. The bracing connection, essentially a fillet welded end connection of a structural tube, appeared to generate marked flexing of the pad plates used in the connection. This detail is probably sensitive to the relative stiffness of the various elements in it.

6. The side sheet to sill connection, tested in simple tension, exhibited both the effects of eccentricity of loading and substantial initial distortion due to the welding process. The relatively small specimens may not be fully representative of the distortions found in the prototype, or of the actual loadings in the side-sheet, which may induce shear and moments on the connection.

2.0 WELDED SPLICES IN TENSION

2.1 GENERAL

This section aggregates for presentation and discussion those welded details for test which can be viewed as member splices for flat elements, primarily in tension. Included in this grouping is Series E, the partial penetration butt weld (shown in Exhibit 2.3). The other joint details include Series I a simple lap splice (shown in Exhibit 2.4), Series J and K a lap splice with a slot weld (shown in Exhibit 2.5), and Series C and D (shown in Exhibit 2.1) which include a plate connected to a portion of the leg of an extruded sill section. With the exception of the partial penetration butt weld, the details included in this grouping possess a lack of axial symmetry which produces an eccentricity of the axial loading on the critical section. This eccentricity is aggravated by welding distortions in some cases--particularly Series C and D.

Finally, Series F is a circular, tubular tension member attached with a simple fillet weld through attachment pads to a chord element. While the chord segment appears as a flexural element, the basic behavior of the detail centers on the fillet weld at the base of the circular tube serving as the member splice. Series F is illustrated in Exhibit 2.6.

For each test series the applied load range for each test is converted to a stress range based on a nominal area of critical material as might be used in the design. It is

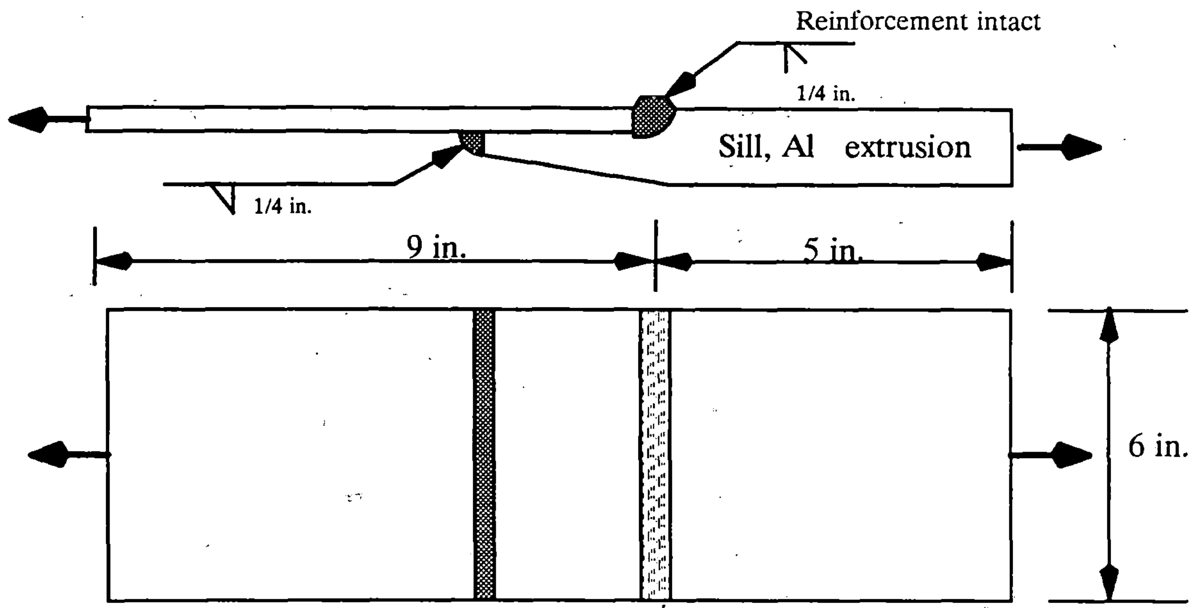

Series C

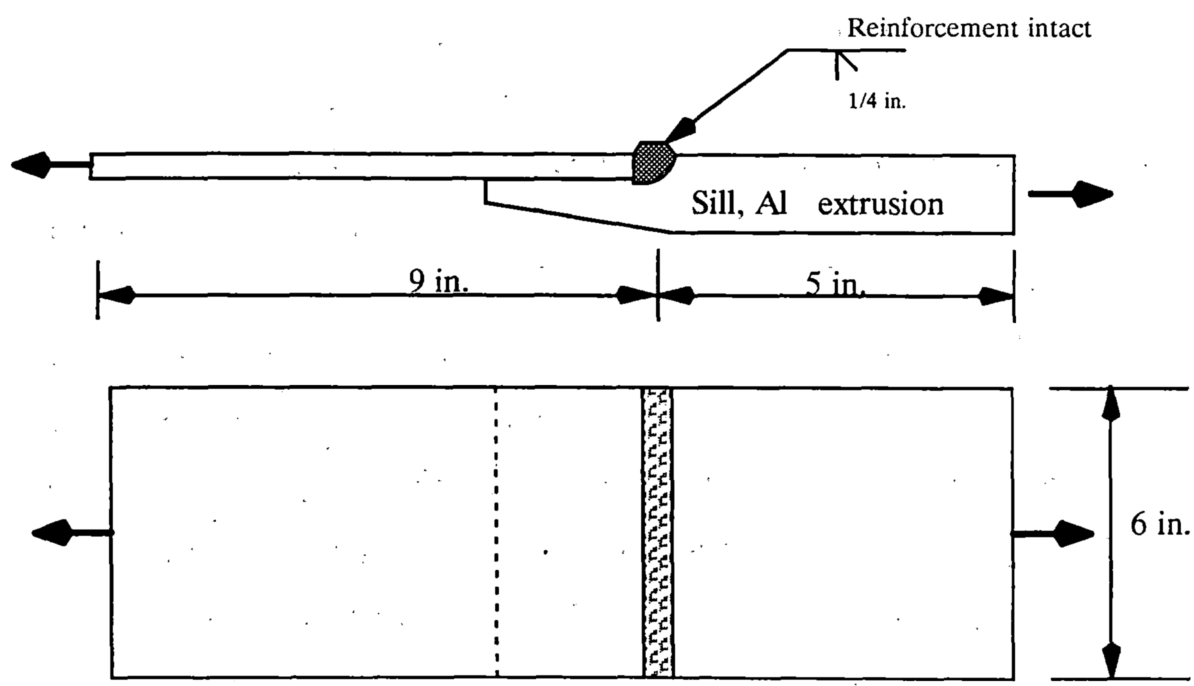

Series D

Exhibit 2.1 Side-Sill Connection Butt Weld With and Without Fillet Weld Series C and D.

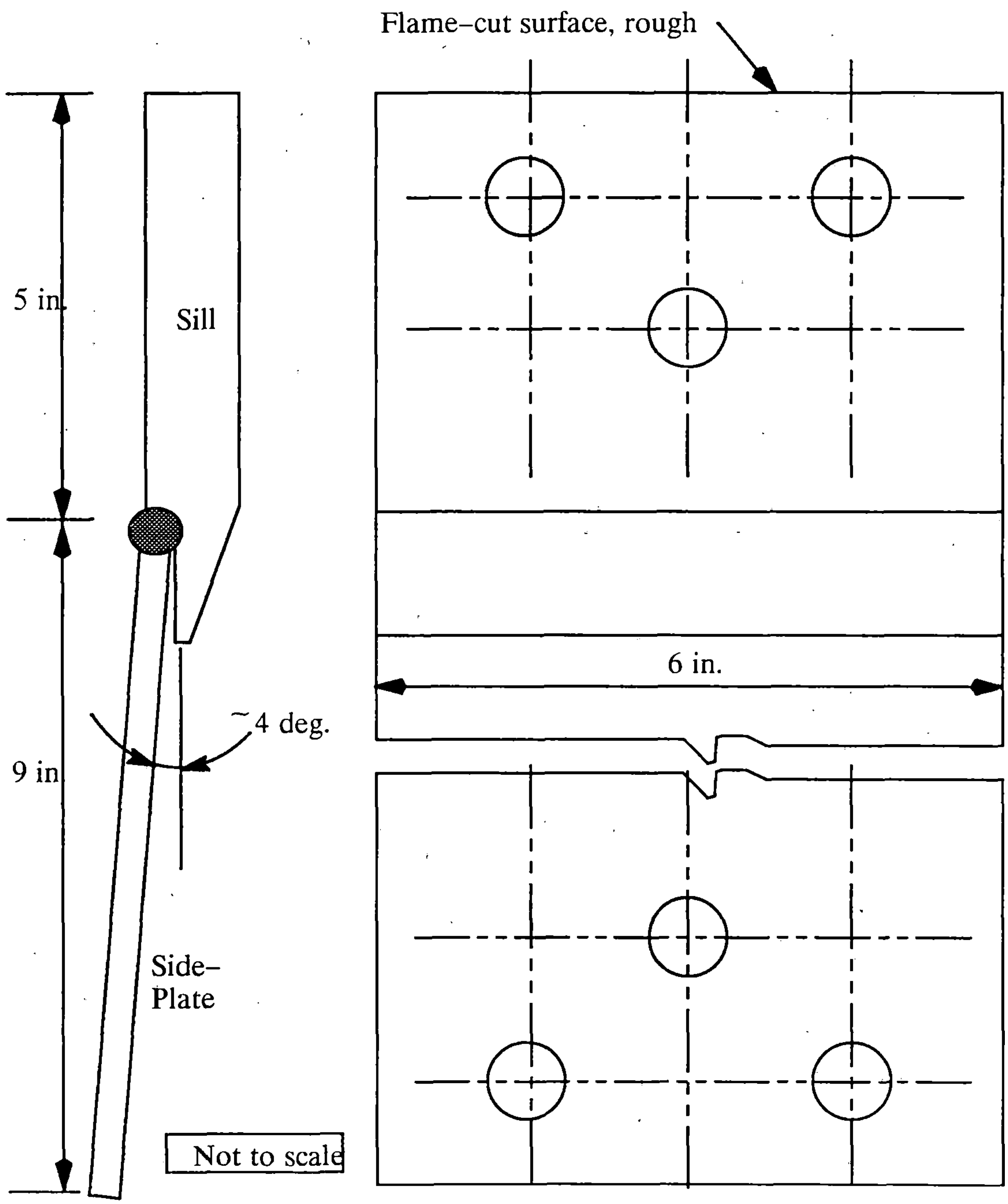

Exhibit 2.2 Series D Test Specimen: Drilled for Pull-Plate Attachment Sketch of Welding Distortion.

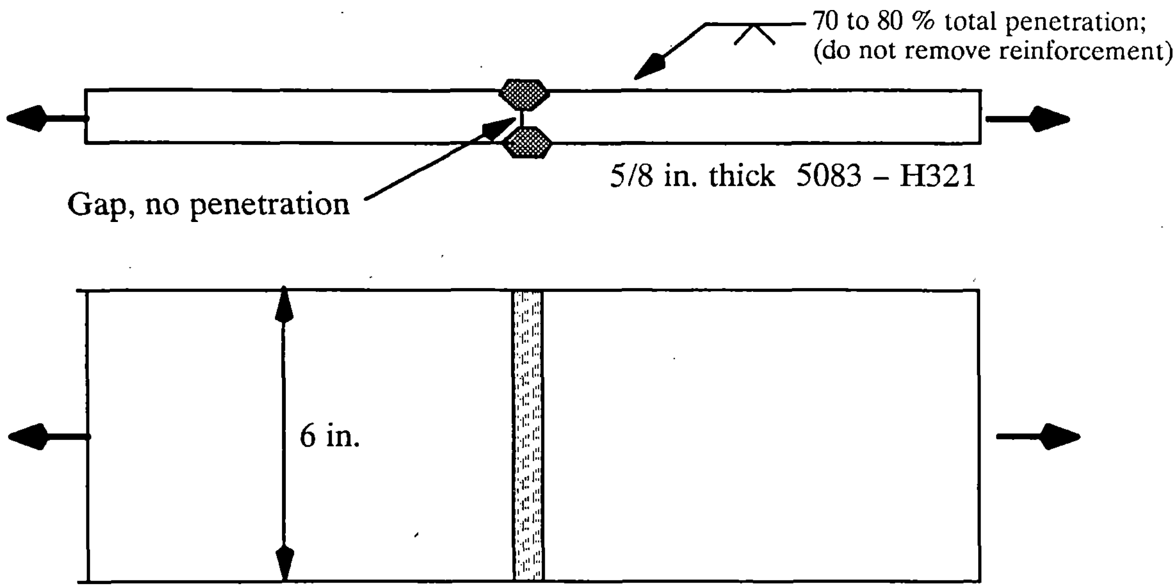

Exhibit 2.3 Partial Penetration Butt Welded Joint--Series E.

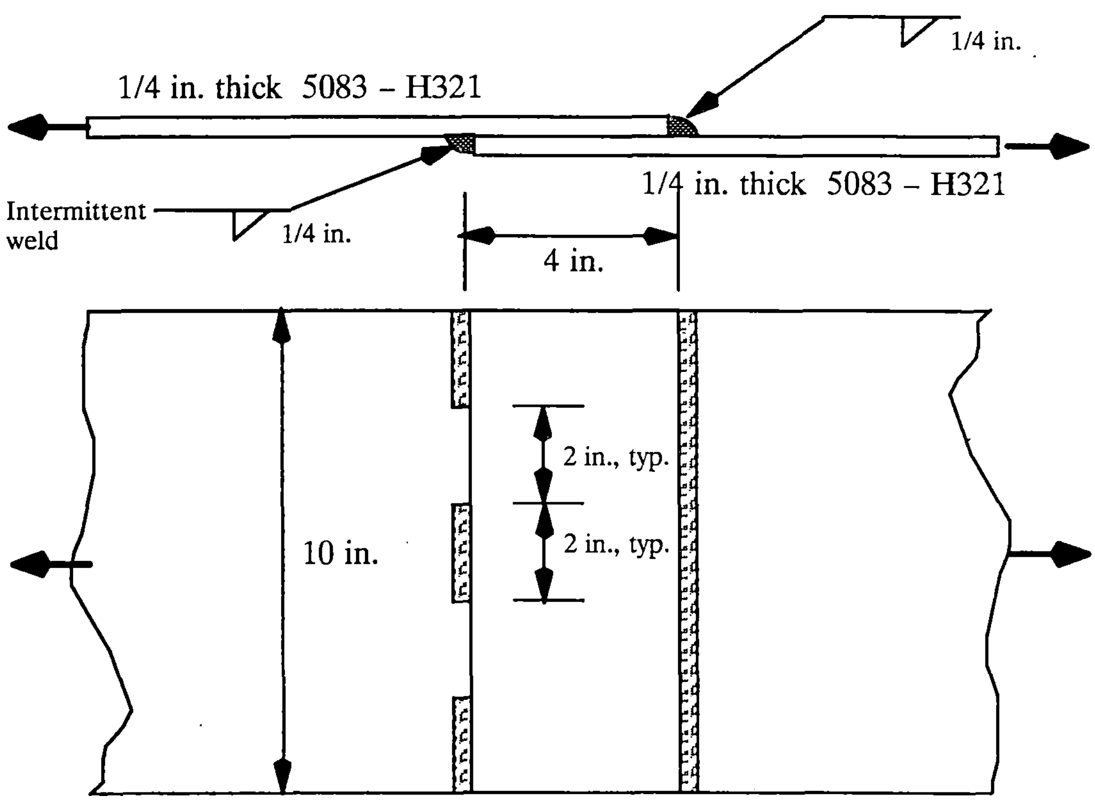

Exhibit 2.4 Fillet Welded Lap Joint with Full and Intermittent Welds Series I.

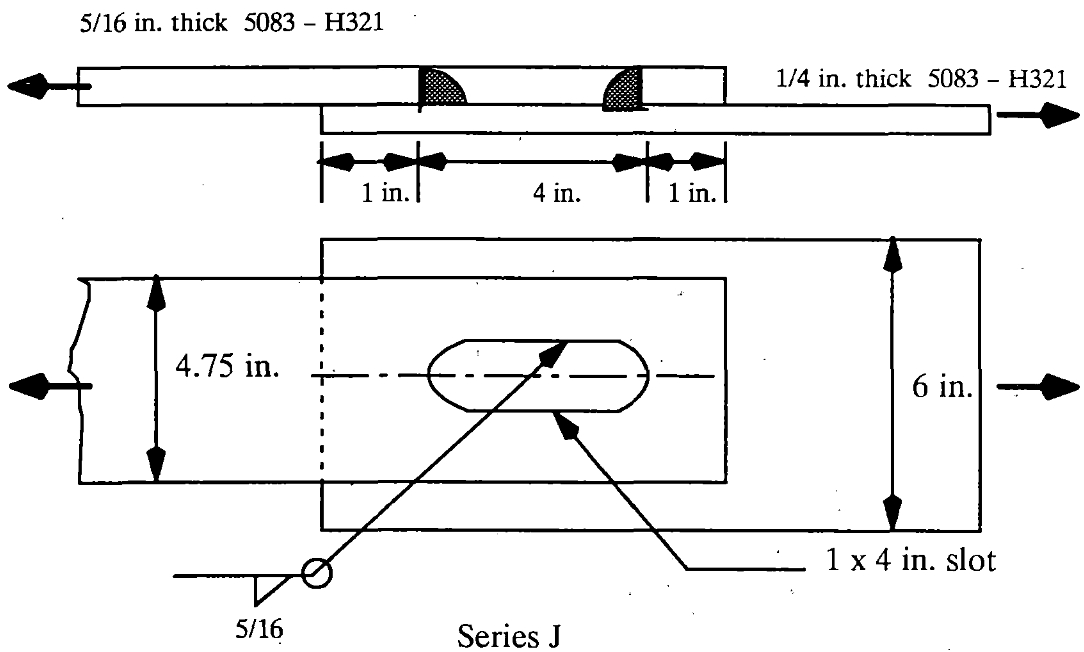

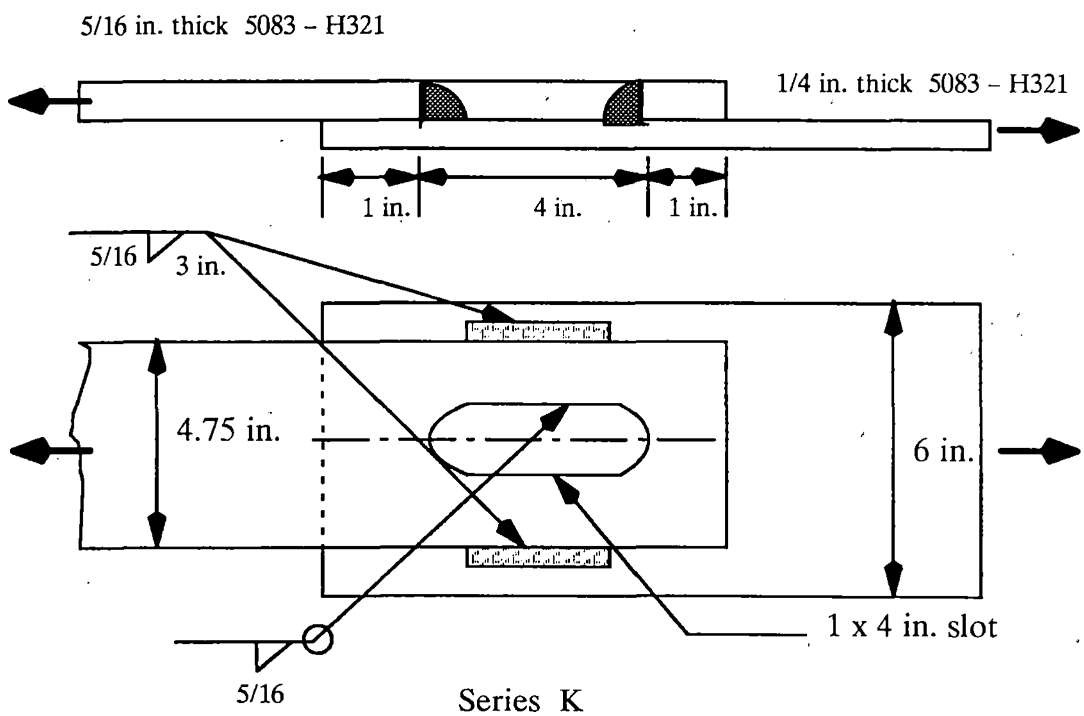

Exhibit 2.5 Welded Slot-Lap Joint With and Without Side Fillet Weld Series J and K.

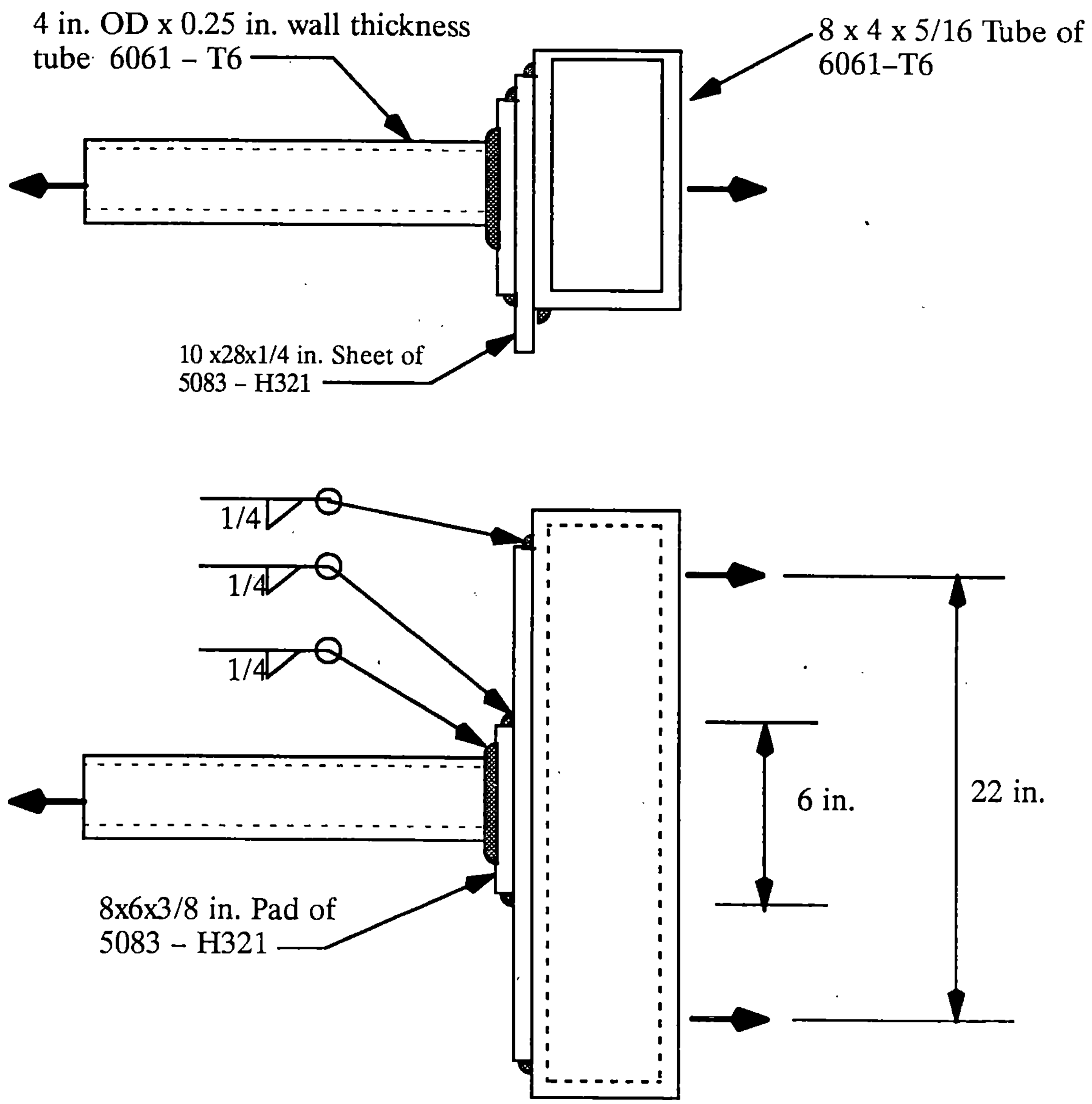

Exhibit 2.6 Welded Diagonal Brace to Top Chord Connection (Simulated) Series F.

important to keep in mind that the flexural components of stress introduced by the eccentricity of the axial load relative to the critical locations for crack initiation and propagation may be large. Thus the nominal stress (Load/$A_{nominal}$) may not be at all representative of the operative state of stress.

2.2 TEST ARRANGEMENTS

The tests presented in this section, with the exception of Series E and F, were conducted in a simple tension loading frame of either 100 kip or 50 kip capacity. At times, two test series were run concurrently. Since the plate widths, 6" to 10" exceed the capacity of the grips available, all specimens (except Series E and F) were drilled for attachment to pull-plates using high-strength A-325 bolts. Series E was tested full-width in the 600 kip capacity loading frame which has grips capable of handling the 6"x 5/8" plate. In no instance did a failure develop at the point of attachment to a pull plate.

Cyclic loads were applied with the system in load control and a deflection limit was set to shut down load cycling at failure. With the modest load requirements in these tests, cycling rates of 4 or 5 Hz were used.

The fittings for the load attachment for Series F are shown in Exhibit 2.7. The chord element was attached to the lower head casting of the 600 kip loading frame with hold-down bars near the ends of the chord segment. The hold-down bolts were secured in existing threaded holes in the head casting and were spaced at 22" on center (see Exhibit 2.7). Tension was applied to the tubular tension member by means of a solid mandrel which was slipped into the tube at its free end and secured with a single high strength bolt. The mandrel projecting from the tube had machined flat surfaces to be clamped in the upper grip of the loading frame. No distress was observed adjacent to any of the loading fittings.

2.3 PRESENTATION OF FATIGUE DATA

The results of the tests are summarized in Tables 2.1 through 2.7 and in the S-N Diagrams presented in Exhibits 2.8 through 2.15. For the S-N Diagrams linear regression lines are shown which are truncated for the range of the data. These regression lines are used to make more extended projections in Section 6. This full set of data and plots must be compared with caution because each class of specimen has distinctly different potentials for eccentricity of loading and the interpretation of the nominal stress must be made with care.

Specific commentary on the mode of failure, location of cracks, etc. is presented in the following section.

2.4 COMMENTARY

Series C and D (See Tables 2.1 and 2.2 and Exhibits 2.5 and 2.6): For Series C the presence of the fillet weld greatly

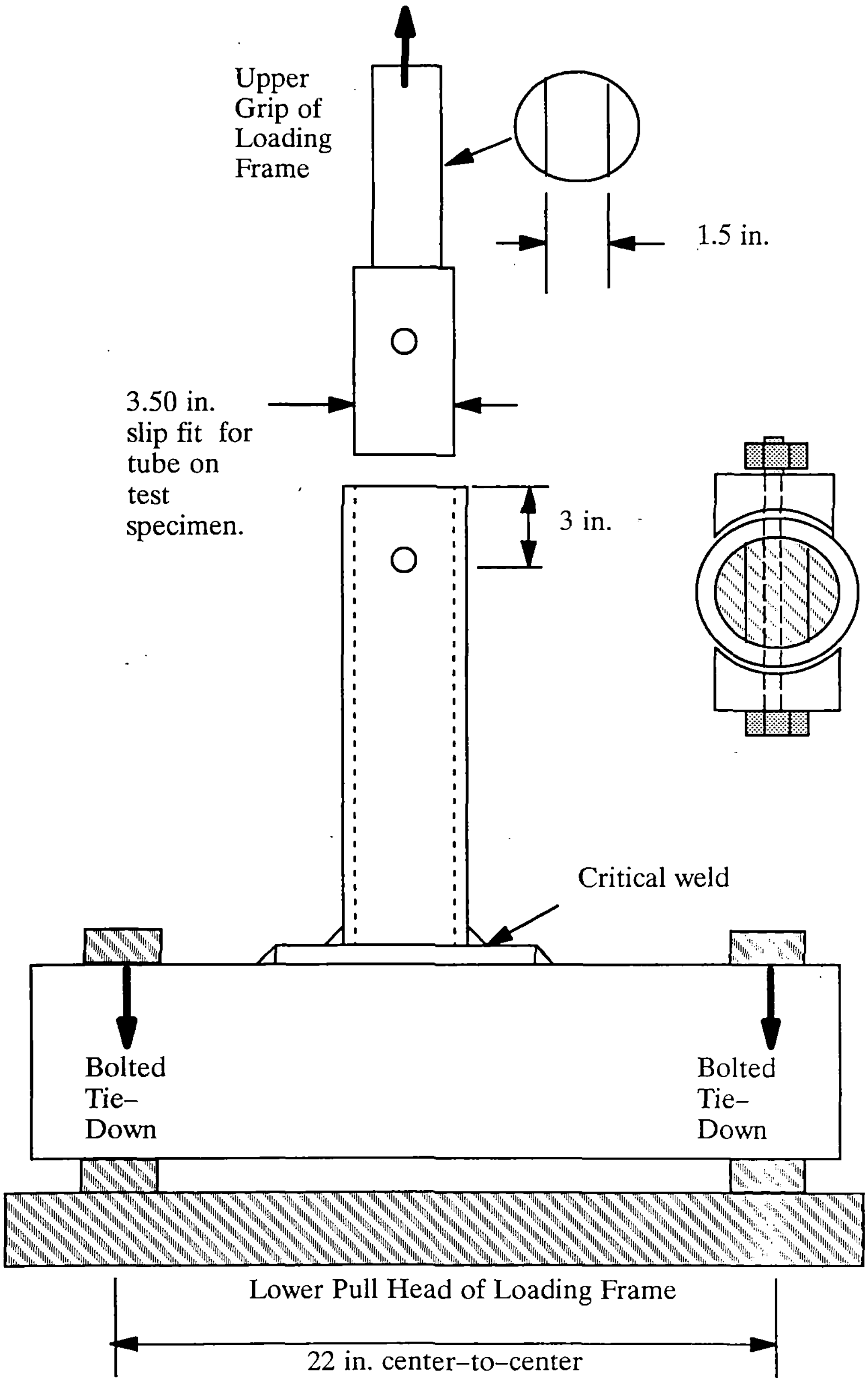

Exhibit 2.7 Fittings for Series F Test.

Table 2.1 Test Results for Series C Welded Side-Sheet to Sill Connection.

(Nominal area = 1.50 in.^{2})

Number	Load Range (kips)	Stress Range (ksi)	Cycles to Failure 1000's	Notes	Plot Symbol
1	11	7.33	646.15	R = 0	Open Triangle
2	12	8.00	496.60	R = 0	Open Triangle
3	8	5.33	1406.80	R = 0	Open Triangle
4	7	4.67	2020.42	R = 0	Open Triangle
5	13	8.67	751.89	R = 0	Open Triangle
6	12	8.00	943.00	R = 0	Open Triangle

Table 2.2 Test Results for Series D Welded Side-Sheet to Sill Connection; Butt Weld Only.

(Nominal area = 1.50 in.^{2})

Number	Load Range (kips)	Stress Range (ksi)	Cycles to Failure 1000's	Notes	Plot Symbol
1	6	4.00	2032.77	R = 0	Open Triangle
2	9	6.00	280.21	R = 0	Open Triangle
3	10	6.67	244.06	R = 0	Open Triangle
4	6	4.00	2589.00	R = 0	Open Triangle
5	7.5	5.00	656.04	R = 0	Open Triangle
6	7.5	5.00	1130.94	R = 0	Open Triangle
7	7.5	5.00	898.55	R = 0	Open Triangle

Table 2.3 Test Results for Series E Partial Penetration Butt Weld.

(Nominal area = 3.75 in.^{2})

Number	Load Range (kips)	Stress Range (ksi)	Cycles to Failure 1000's	Notes	Plot Symbol
1	38	10.13	33.47	R = 0	Open Triangle
2	19	5.07	559.18	R = 0	Open Triangle
3	19	5.07	478.61	R = 0	Open Triangle
4	38	10.13	25.20	R = 0	Open Triangle
5	15	4.00	953.23	R = 0	Open Triangle
6	14	3.73	1434.03	R = 0	Open Triangle
7	40	8.00	113.50	R = 0	Open Triangle
8	13.5	3.60	3800	R = 0	Run-out,Solid Triangle

Table 2.4 Test Results for Series I Welded Single Lap Splice.

(Nominal area = 2.50 in.^{2})

Number	Load Range (kips)	Stress Range (ksi)	Cycles to Failure 1000's	Notes	Plot Symbol
1	28	11.20	14.08	R = 0	Open Triangle
2	14	5.60	116.20	R = 0	Open Triangle
3	7	2.80	2018.00	R = 0	Open Triangle
4	14	5.60	119.00	R = 0	Open Triangle
5	7	2.80	1689.59	R = 0	Open Triangle
6	24	9.60	13.79	R = 0	Open Triangle
7	9	3.60	397.51	R = 0	Open Triangle
8	9	3.60	456.50	R = 0	Open Triangle

Table 2.5 Test Results for Series J Slot-Welded Lap Splice.

(Nominal area = 1.50 in.^{2})

Number	Load Range (kips)	Stress Range (ksi)	Cycles to Failure 1000's	Notes	Plot Symbol
1	7	4.67	113.16	R = 0	Open Triangle
2	7	4.67	97.09	R = 0	Open Triangle
3	4	2.67	432.00	R = 0	Open Triangle
4	4	2.67	452.90	R = 0	Open Triangle
5	2.5	1.67	4808.00	R = 0	Open Triangle
6	3	2.00	3099.05	R = 0	Open Triangle

Table 2.6 Test Results for Series K Slot-Welded Lap Splice with Side Fillet Welds.

(Nominal area = 1.50 in.^{2})

Number	Load Range (kips)	Stress Range (ksi)	Cycles to Failure 1000's	Notes	Plot Symbol
1	7	4.67	145.00	R = 0	Open Triangle
2	7	4.67	166.60	R = 0	Open Triangle
3	4	2.67	577.20	R = 0	Open Triangle
4	4	2.67	639.70	R = 0	Open Triangle
5	3	2.00	1177.56	R = 0	Open Triangle
6	3	2.00	3870.56	R = 0	Open Triangle

Table 2.7 Test Results for Series F Brace to Top Chord Connection.

(Nominal area = 2.22 in.^{2})

Number	Load Range (kips)	Stress Range (ksi)	Cycles to Failure 1000's	Notes	Plot Symbol
1	5	2.25	675.00	R = 0	Open Triangle
2	6.5	2.93	175.00	R = 0	Open Triangle
3	6.5	2.93	77.00	R = 0	Open Triangle
4	4.5	2.03	591.00	R = 0	Open Triangle
5	4.5	2.03	540.00	R = 0	Open Triangle
6	3.8	1.71	738.30	R = 0	Open Triangle
7	10	4.50	0.30	R = 0	Not Plotted

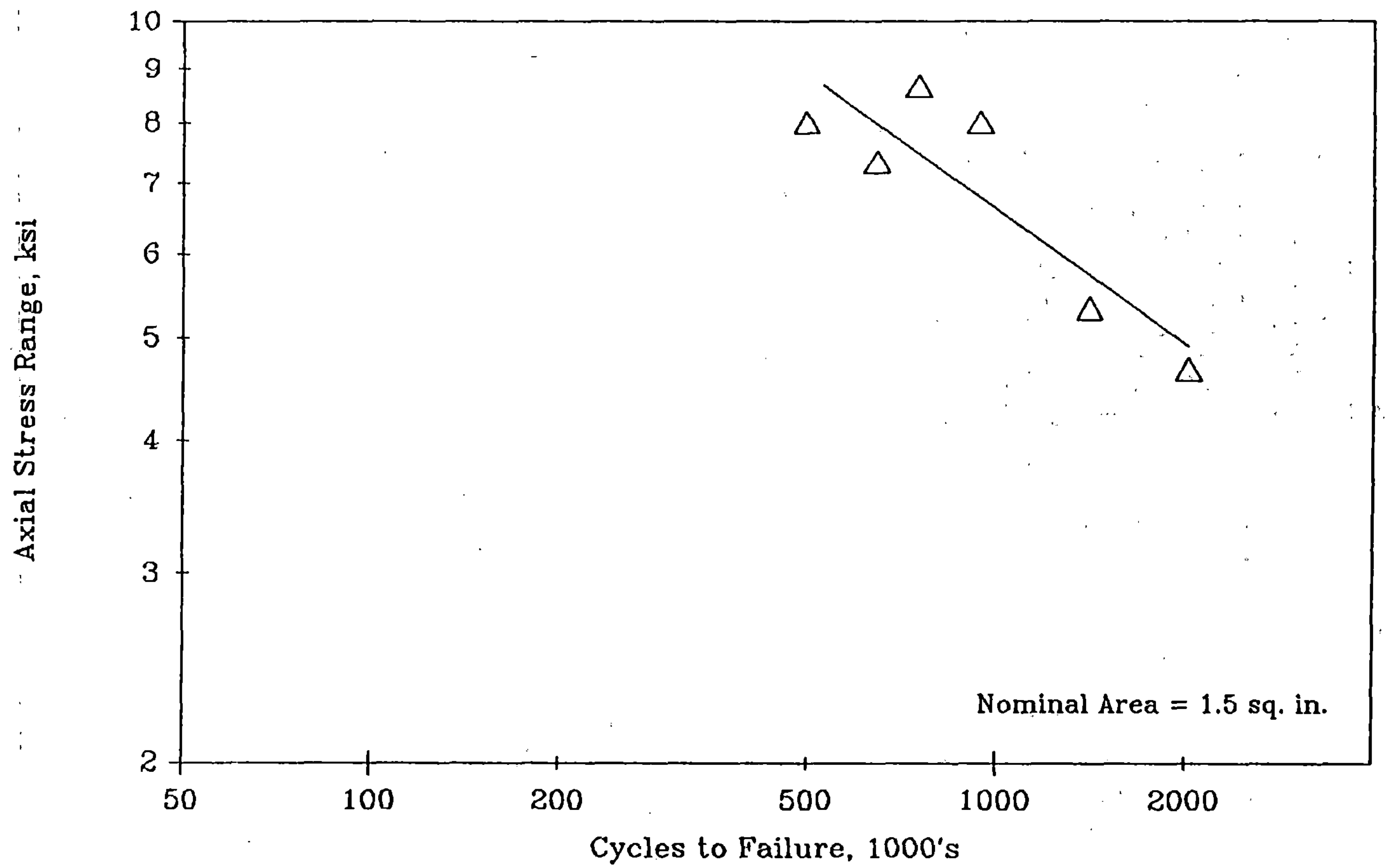

Exhibit 2.8 S-N Diagram for Series C--Sill Connection with Butt Weld and Fillet Weld.

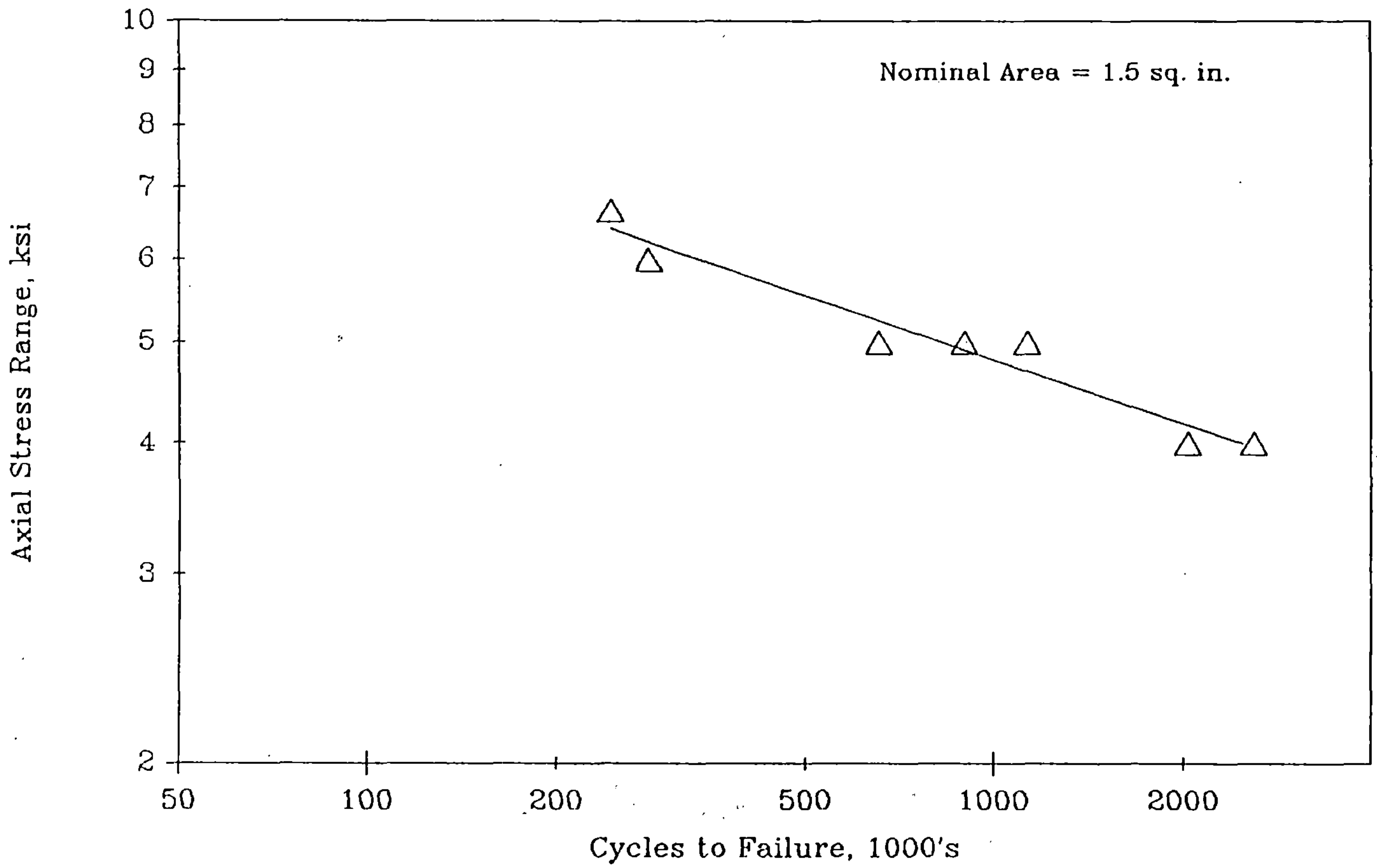

Exhibit 2.9 S-N Diagram for Series D--Sill Connection with Butt Weld.

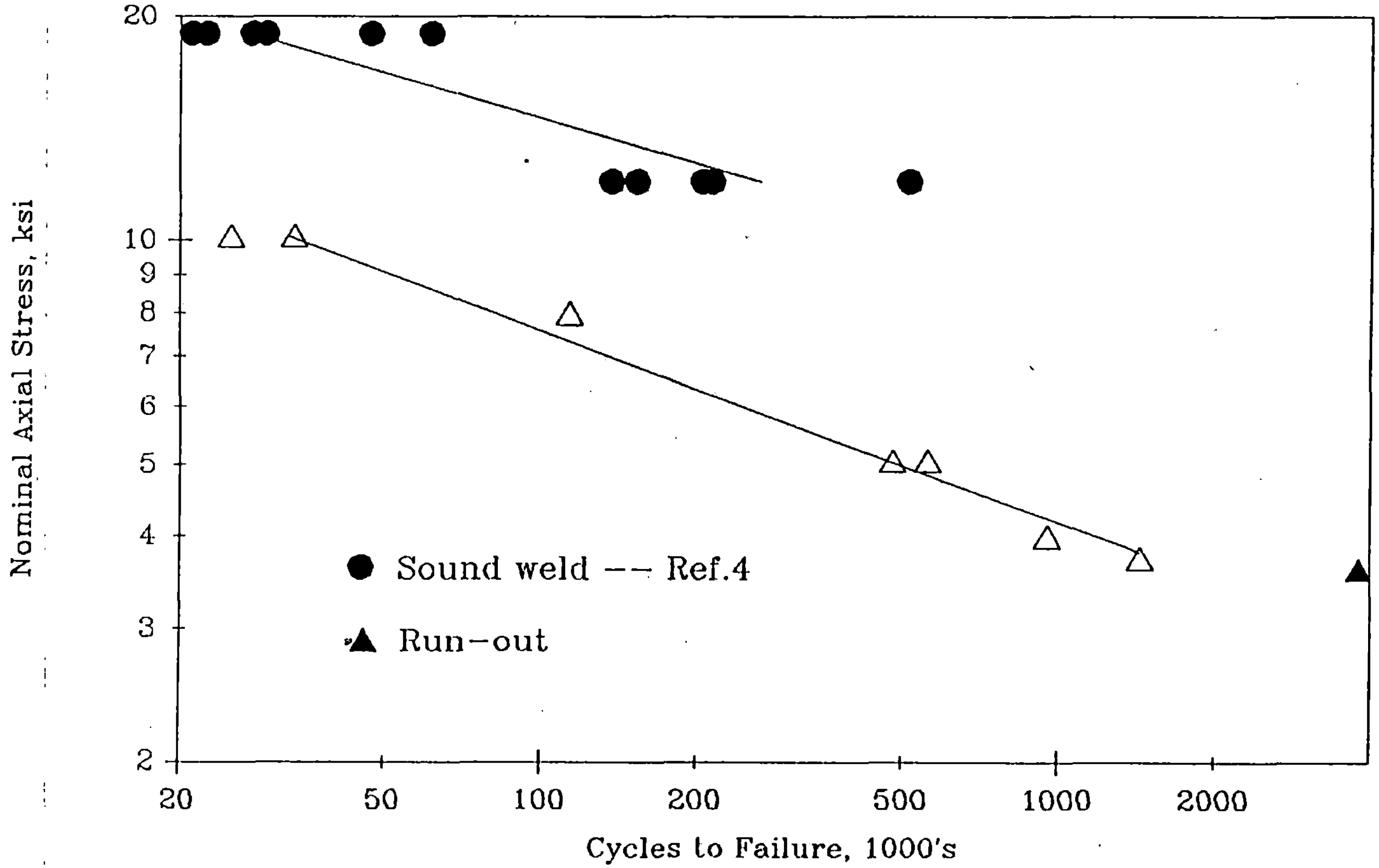

Exhibit 2.10 S-N Diagram for Series E--Partial Penetration Butt Weld.

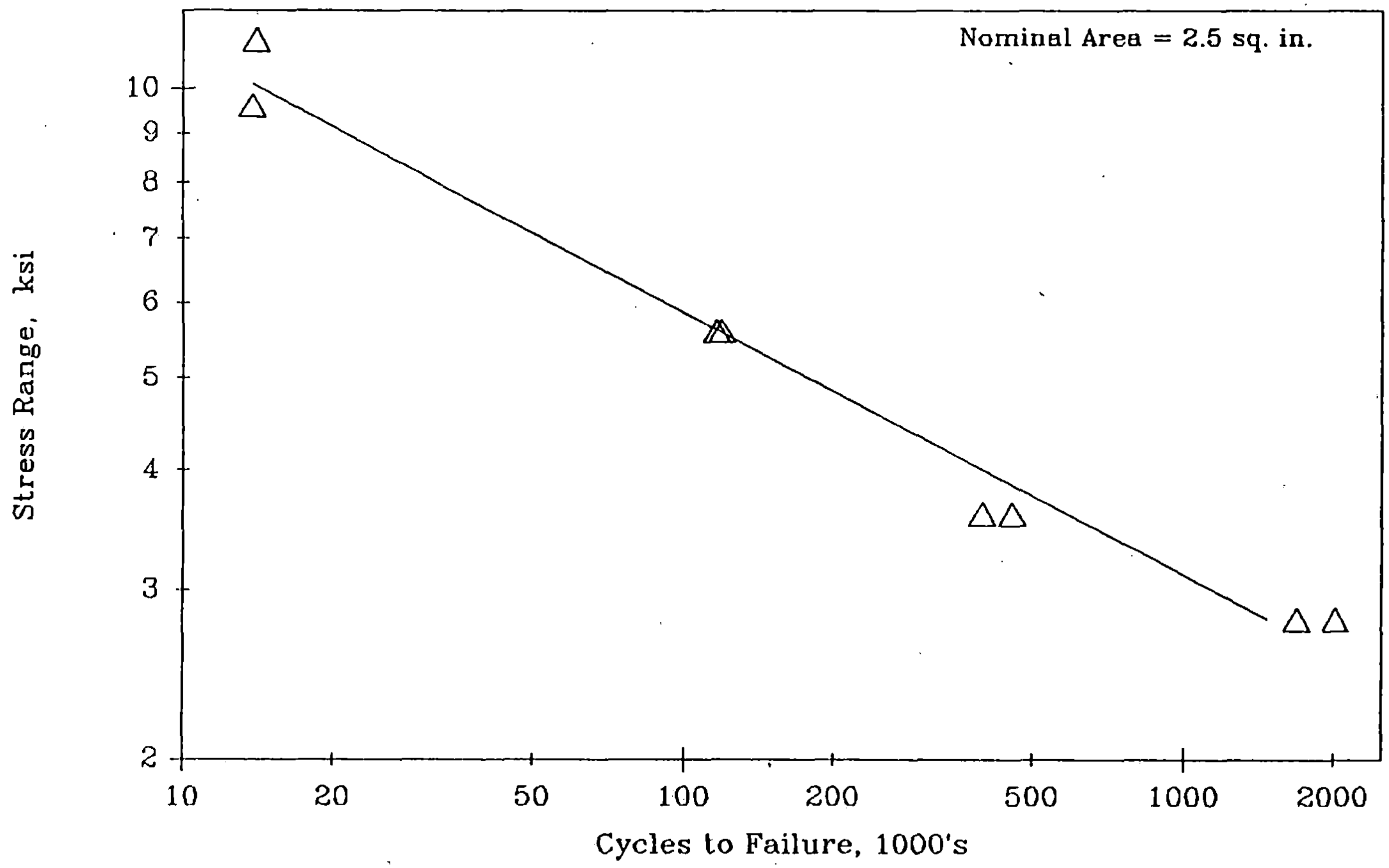

Exhibit 2.11 S-N Diagram for Series I--Welded Lap Splice.

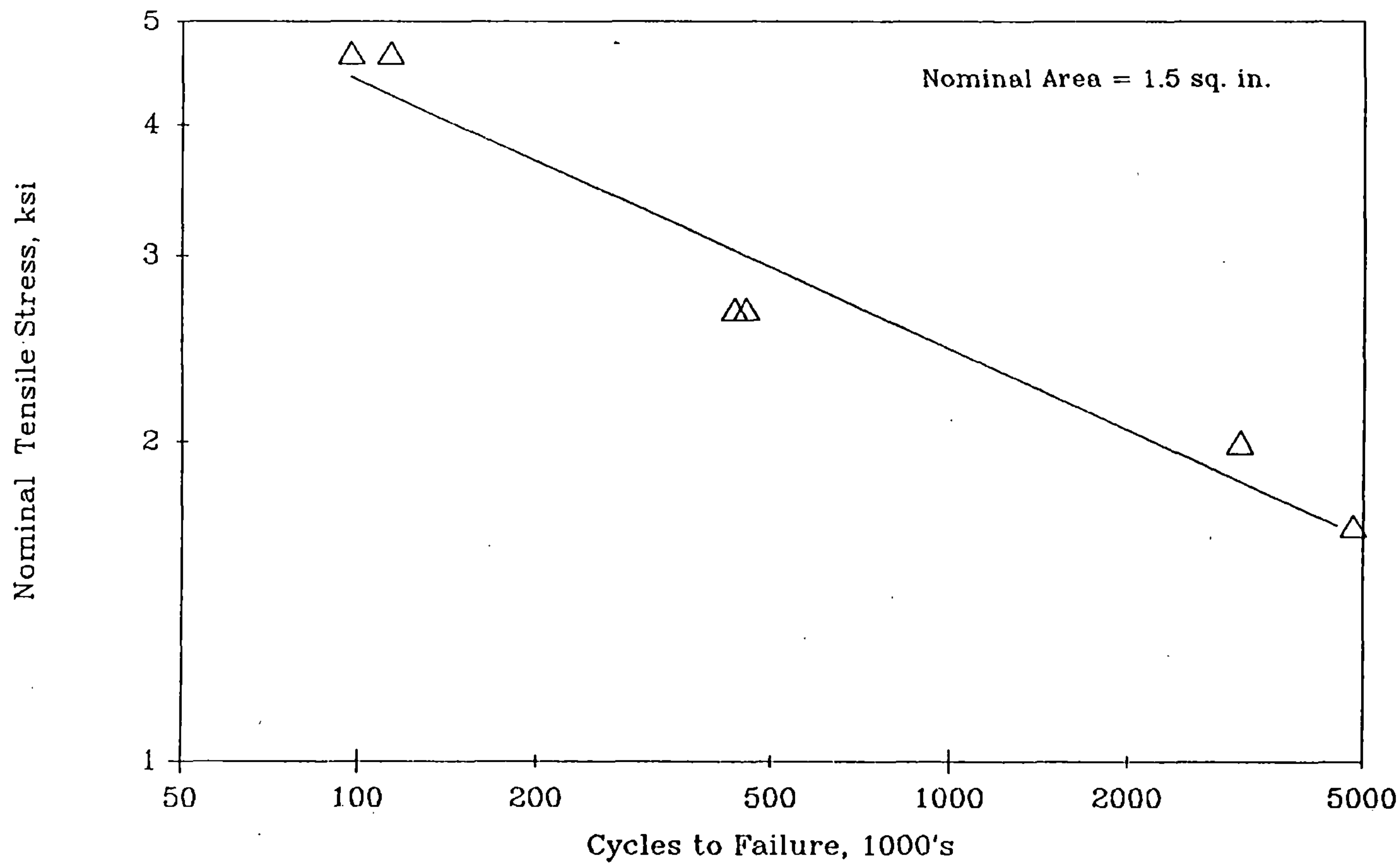

Exhibit 2.12 S-N Diagram for Series J--Slot Welded Lap Splice Without Side Welds.

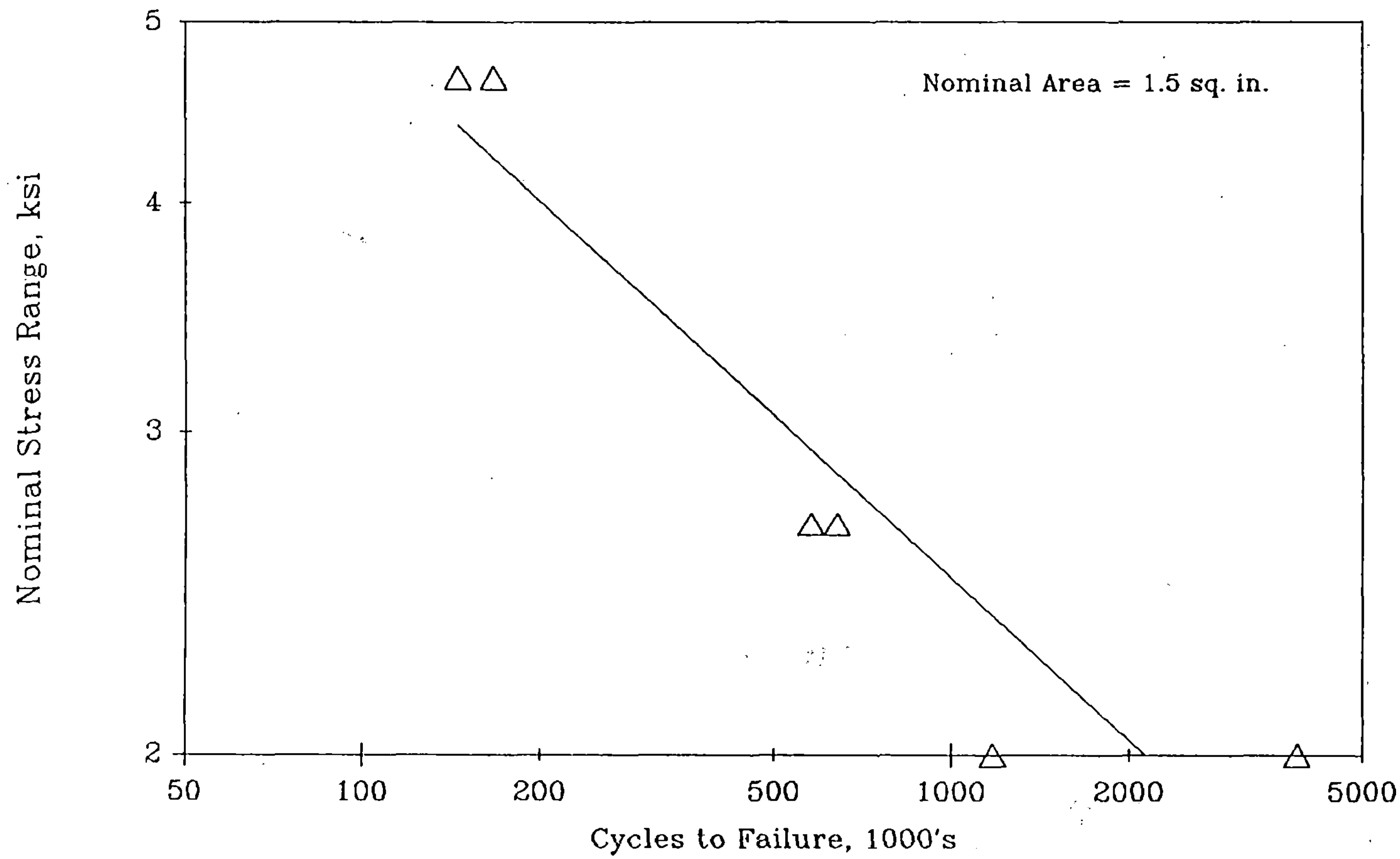

Exhibit 2.13 S-N Diagram for Series K--Slot Welded Lap Splice With Side Welds.

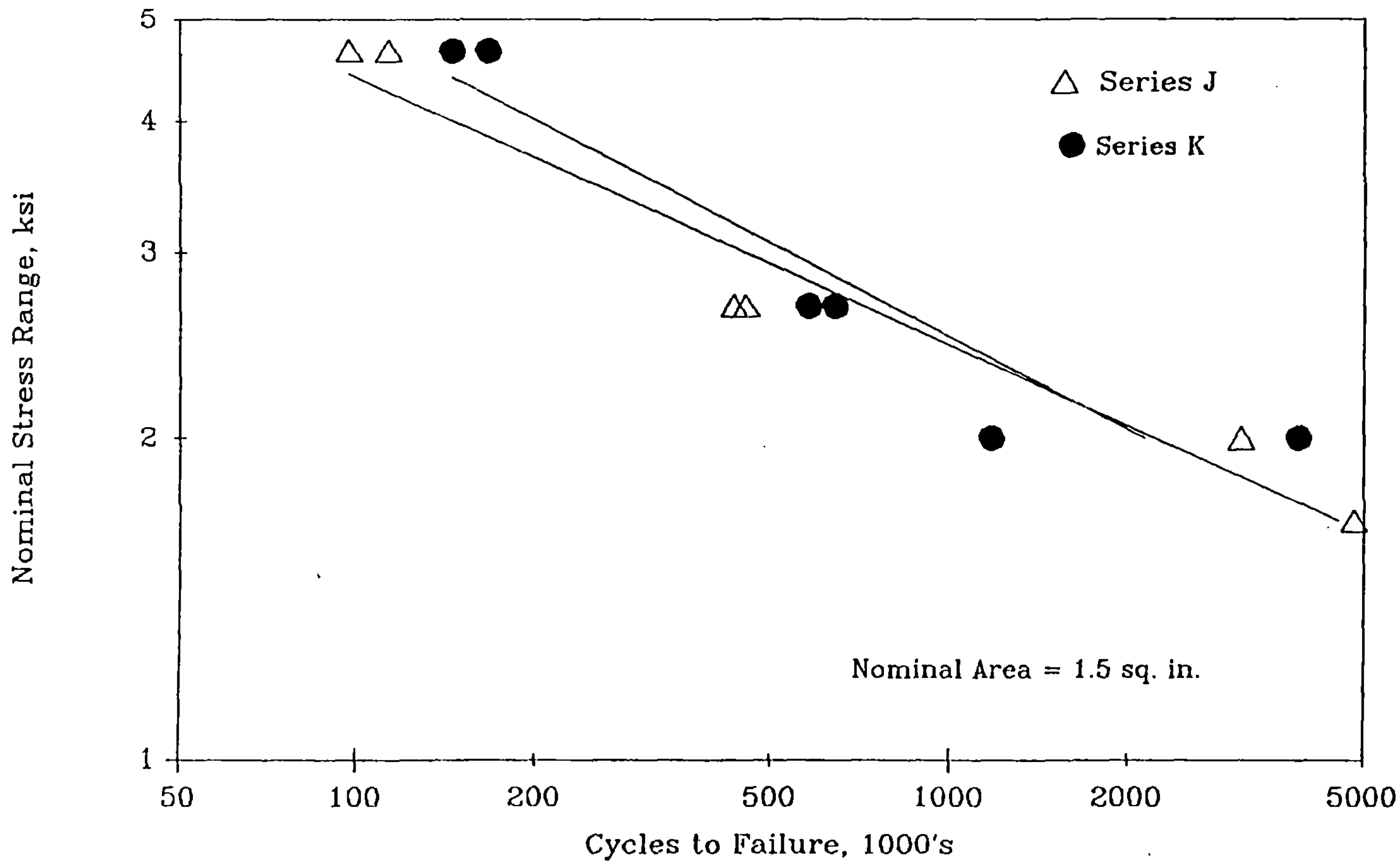

Exhibit 2.14 Comparison of S-N Diagrams for Series J and K.

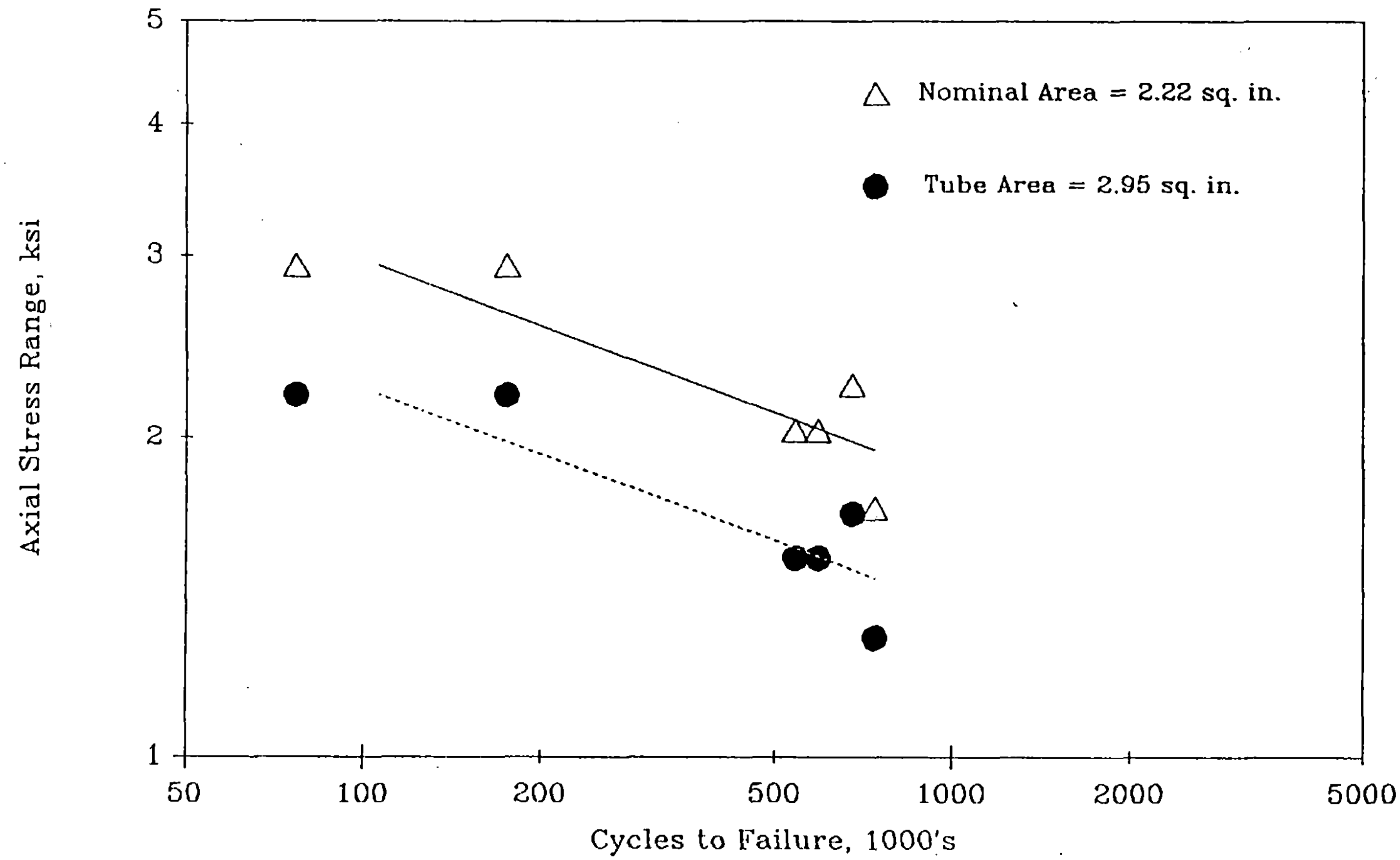

Exhibit 2.15 S-N Diagram for Series F--Brace to Top Chord Connection.

reduced distortion in the joint in contrast to Series D -- see Exhibit 2.2. The presence of the welding distortion made shimming the specimen in the load frame grips difficult; no attempt was made to use tapered shims to accommodate the initial angular distortion. After loading for a substantial portion of the life of the specimen, the distortion is reduced, and for one test where the cycling was stopped before full propagation of the crack across the section, the angular distortion is essentially absent from the specimen when removed from the test fixtures.

The load capacities of these two details did not differ markedly; the test loads ranging from 13 to 7 kips for Series C and 10 to 6 kips for Series D. In all instances the fatigue cracking is associated with plate material immediately adjacent to the welds. The nominal areas of weld were 2.56 and 1.50 in.^{2}, respectively for Series C and D. The slope of the regression lines differ markedly and over a broad range of total life the data for these series overlap.

Series E (Table 2.3 and Exhibit 2.7): The fracture surfaces of the failed specimens for Series E showed consistency in obtaining about 80 percent penetration of the weld. The weld reinforcement was allowed to remain intact. The characteristic area for this series was the gross area of the plate. Included in Exhibit 2.7 are data taken from Ref. 4 for 5083 aluminum welds, made in 3/8 in. thick material, which have been found to have full penetration. The regression lines are nearly parallel and the degradation in strength due to the partial penetration weld is distinct -- on the order of a factor of two.

<u>Series I:</u> During load cycling, the effect of eccentricity in this simple lap joint was apparent. The cracking was always associated with the termination of a fillet weld and propagated under the influence of the substantial flexural stress component in combination with the nominal axial stress. The S-N diagram is characterized by a low degree of scatter.

<u>Series J and K:</u> These tests share the influence of the slot weld and flexural stress due to eccentricity of loading. The fatigue failure most often started at the stress concentration associated with the end of the slot weld and would propagate through the adjacent stress plate and then as a through crack across the width of the specimen. The addition of the side fillet welds in Series K did not markedly improve the load carrying capacity. The apparent failure stresses were reduced because of the increase in nominal area of the weld. Results for the two series are compared in Exhibit 2.14.

<u>Series F:</u> The critical weld in this detail is the fillet weld placed around the junction of the tube brace and the first pad in the attachment (see Exhibit 2.7). The fatigue failure always initiated in this weld and would propagate partially around the circumference by at least 90 degrees. Additional crack growth out into the pad or in the fillet

welds attaching the pads would ensue. The flexing of the relatively thin pads was clearly visible during the tests. No distress in the main chord member was observed.

3.0 BOLTED TENSION SPLICES

3.1 GENERAL

Series A and B are bolted tension splices with the bolts loaded in single and double shear, respectively. In Exhibit 3.1 the arrangement of the joints and placement of the bolts as specified by the VTS Committee is shown; as will be noted subsequently, the specimens were machined to achieve a reduced critical net section. All specimens had four standard 5/8 in. diameter Huck bolts. The connections in every case were of a proportion such that failure occurred in the connected elements and not in the bolts. All specimens were comprised of a steel plate connected to one (Series A) or two (Series B) aluminum plates; a mastic was used on the facing surfaces to inhibit corrosion. The original specification called for a 5/16 in. aluminum plate in Series B, but a 1/4 in. plate was supplied; similarly the aluminum plate in Series A was reduced to a 1/2 in. thickness.

The original test plan called for a full reversal tests for the Series A and B program. However, the 1/4 in. aluminum plate sections had a radius of gyration of only 0.0722 in., a slenderness ratio of over 124, and thus a buckling stress on the order of 6.3 ksi. Operating at loads near the critical buckling stress also would drastically increase the flexural effects due to eccentricity because of moment amplification under compression loading. The test program was revised to

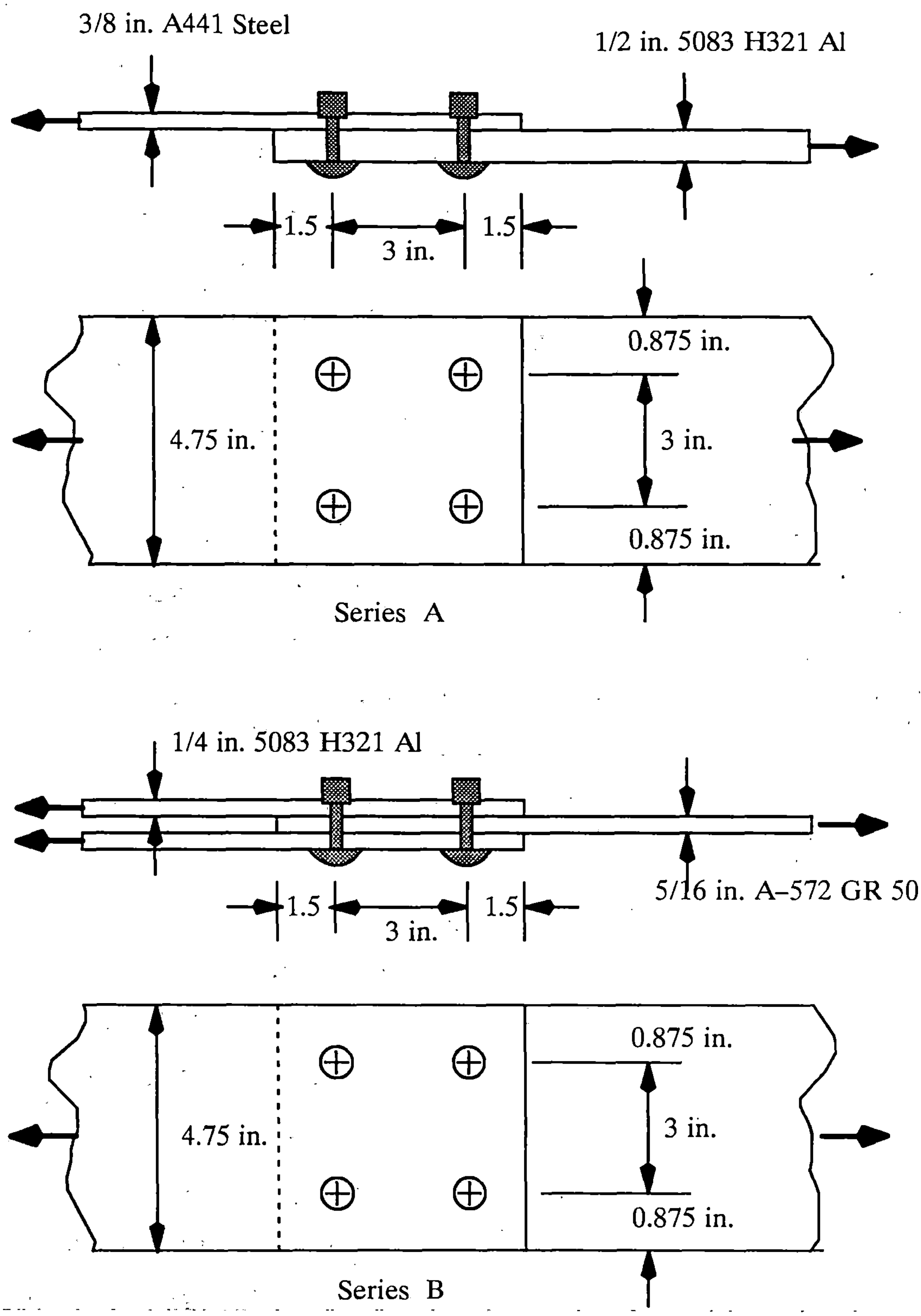

Exhibit 3.1 Bolted Lap Joints in Single and Double Shear--Huck Bolts Series A and B.

increase tests run for R = 0 and 0.5.

The test program was also modified to include two methods of specimen fabrication: holes punched and holes sub-punched and reamed.

3.2 TEST ARRANGEMENT

All tests were conducted in the 800 kip load frame in Newmark Laboratory. This machine was chosen because the available width of grip permitted the 6 in. wide plates to be pulled without fixtures or modification. It proved to be impossible to test the delivered specimens in the original geometry with a full 6 in. width at the net section level; such a procedure nearly always induces failure in the machine grips. All tests reported herein were conducted on specimens cut to the reduced section shown in Exhibit 3.2, that is, a gross width at the critical section of 4.75 in. The width reduction left an edge distance of 0.875 in. or 1.4 times the fastener diameter. This appears to be an acceptable level in a direction perpendicular to the direction of loading. For steel structures, a minimum edge distance of 7/8 in. is specified (AISC-ASD Specification) for 5/8 in diameter fasteners for all forms of edge preparation except shearing.

3.3 PRESENTATION OF FATIGUE DATA

The data for Series A and B is presented in four tabulations, Tables 3.1 through 3.4, and in the S-N Diagrams

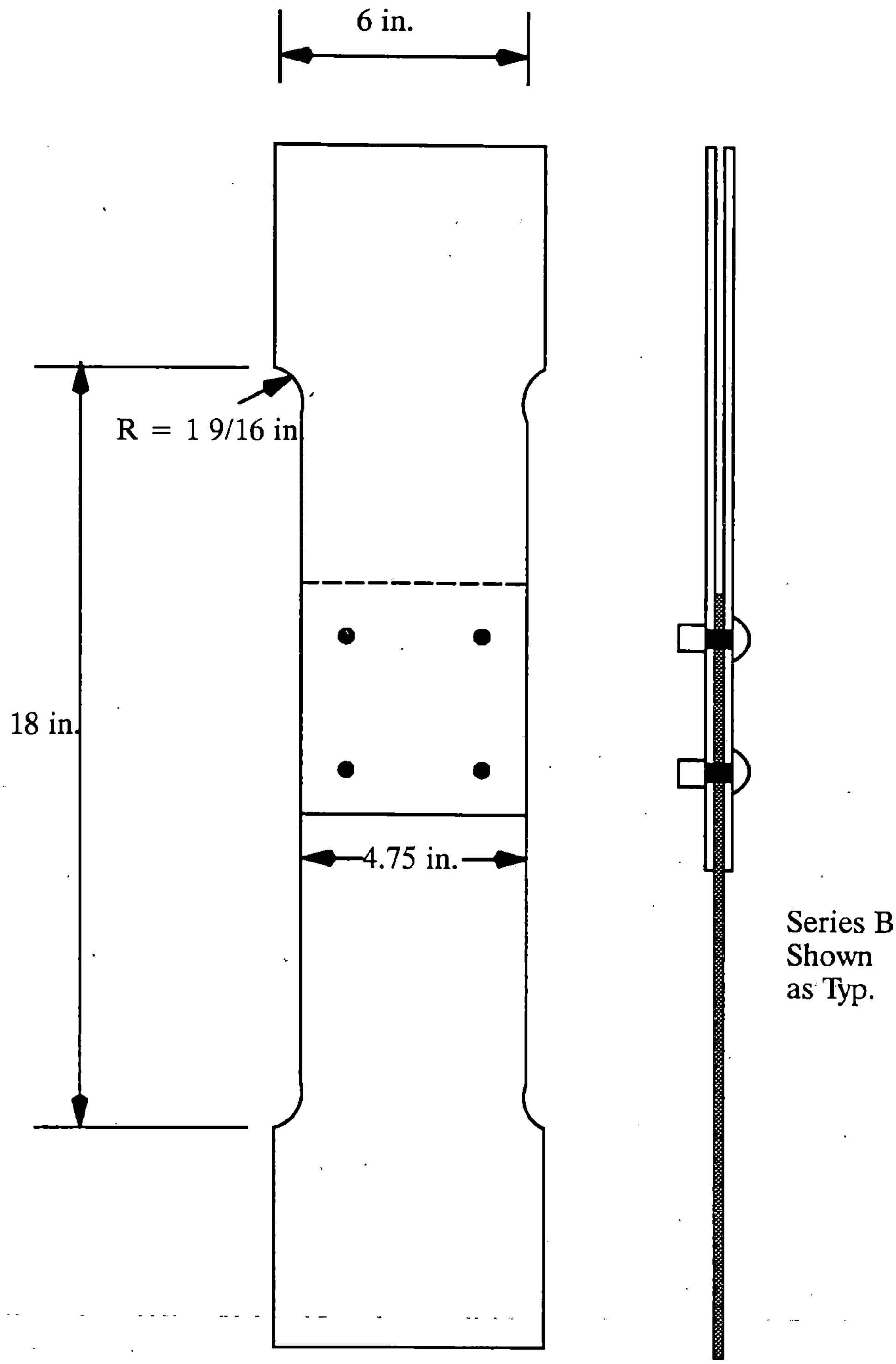

Exhibit 3.2 Sketch of Trimming for Reduced Net Section for Series A and B.

Table 3.1 Test Results for Series A Huck-Bolted Lap Splice with Punched Holes.

(Nominal area = 1.6875 in.^{2})

Number	Load Range (kips)	Stress Range (ksi)	Cycles to Failure 1000's	Notes	Plot Symbol
1	40	23.70	15.64	R = 0	Open Triangle
2	20	11.85	469.74	R = 0	Open Triangle
3	20	11.85	490.50	R = 0	Open Triangle
4	30	17.78	128.84	R = 0	Open Triangle
5	16	9.48	8148.15	R = 0	Open Triangle
6	17	10.07	2285.28	R = 0	Open Triangle
7	15	8.89	5000.00	R = 0	Run-Out,Solid Triangle
8	30	17.78	15.8	R = 0.5	Open Diamond
9	25	14.81	102.31	R = 0.5	Open Diamond
10	20	11.85	211.71	R = 0.5	Open Diamond
11	30	17.78	53.54	R = 0.5	Open Diamond
12	25	14.81	95.36	R = 0.5	Open Diamond
13	20	11.85	243.40	R = 0.5	Open Diamond
14	15	8.89	586.84	R = 0.5	Open Diamond
15	15	8.89	577.69	R = 0.5	Open Diamond
16	30	17.78	36.56	R = 0.5	Open Diamond
17	12	7.11	781.37	R = 0.5	Open Diamond

Table 3.2 Test Results for Series A Huck-Bolted Lap Splice with Reamed Holes.

(Nominal area = 1.6875 in.^{2})

Number	Load Range (kips)	Stress Range (ksi)	Cycles to Failure 1000's	Notes	Plot Symbol
1	20	11.85	652.79	R = 0	Solid Circle
2	30	17.78	162.64	R = 0	Solid Circle
3	20	11.85	534.36	R = 0	Solid Circle
4	30	17.78	83.26	R = 0	Solid Circle
5	40	23.70	11.28	R = 0	Solid Circle
6	40	23.70	32.75	R = 0	Solid Circle
7	17	10.07	1058.00	R = 0	Solid Circle
8	20	11.85	277.00	R = 0.5	Solid Diamond
9	20	11.85	160.67	R = 0.5	Solid Diamond
10	16	9.48	439.44	R = 0.5	Solid Diamond
11	25	14.81	79.55	R = 0.5	Solid Diamond
12	16	9.48	265.15	R = 0.5	Solid Diamond
13	25	14.81	137.53	R = 0.5	Solid Diamond
14	12	7.11	1051.57	R = 0.5	Solid Diamond
15	12	7.11	984.00	R = 0.5	Solid Diamond

Table 3.3 Test Results for Series B Huck-Bolted Double Lap Splice with Punched Holes.

(Nominal area = 1.6875 in.^{2})

Number	Load Range (kips)	Stress Range (ksi)	Cycles to Failure 1000's	Notes	Plot Symbol
1	45	26.67	154.54	R = 0	Open Triangle
2	30	17.78	736.78	R = 0	Open Triangle
3	30	17.78	1877.46	R = 0	Open Triangle
4	45	26.67	247.86	R = 0	Open Triangle
5	37.5	22.22	452.10	R = 0	Open Triangle
6	37.5	22.22	631.80	R = 0	Open Triangle
7	30	17.78	68.70	R = 0.5	Open Diamond
8	30	17.78	41.38	R = 0.5	Open Diamond
9	27	16.00	1355.71	R = 0.5	Open Diamond
10	27	16.00	698.00	R = 0.5	Open Diamond
11	24	14.22	688.69	R = 0.5	Open Diamond
12	24	14.22	1061.01	R = 0.5	Open Diamond

Table 3.4 Test Results for Series B Huck-Bolted Double Lap Splice with Reamed Holes: R = 0.

(Nominal area = 1.6875 in.^{2})

Number	Load Range (kips)	Stress Range (ksi)	Cycles to Failure 1000's	Notes	Plot Symbol
1	45	26.67	379.85	R = 0	Solid Circle
2	30	17.78	980.50	R = 0	Solid Circle
3	30	17.78	1358.08	R = 0	Solid Circle
4	45	26.67	324.69	R = 0	Solid Circle
5	37.5	22.22	502.95	R = 0	Solid Circle
6	37.5	22.22	714.90	R = 0	Solid Circle
7	30	17.78	353.10	R = 0.5	Solid Diamond
8	30	17.78	317.06	R = 0.5	Solid Diamond
9	37.5	22.22	0.02	R = 0.5	Not Plotted
10	37.5	22.22	0.05	R = 0.5	Not Plotted
11	24	14.22	2350.10	R = 0.5	Solid Diamond
12	27	16.00	732.60	R = 0.5	Solid Diamond
13	33	19.56	96.60	R = 0.5	Solid Diamond
14	33	19.56	42.28	R = 0.5	Solid Diamond
15	27	16.00	633.15	R = 0.5	Solid Diamond

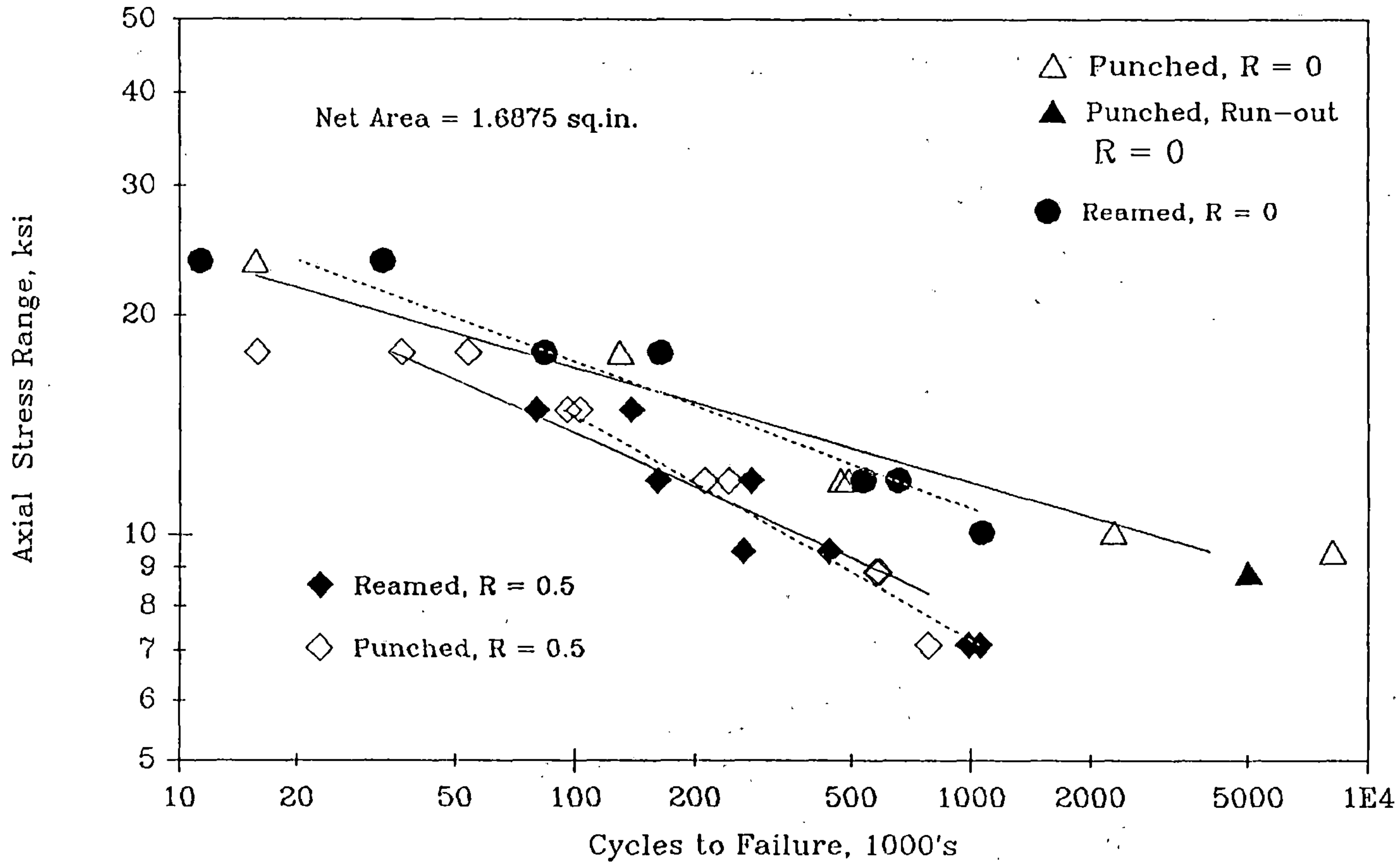

Exhibit 3.3 S-N Diagram for Series A--Single Bolted Lap Splice.

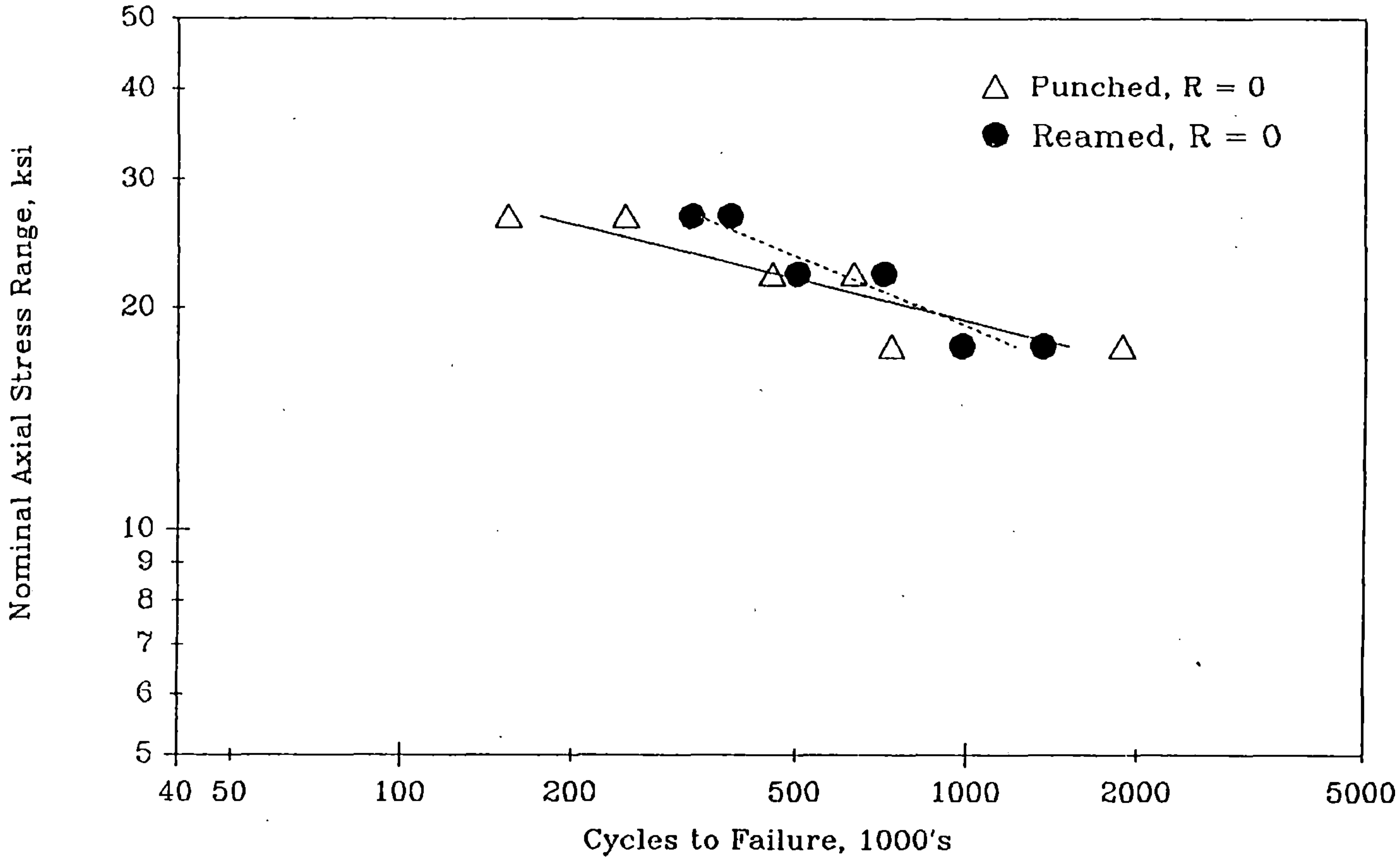

Exhibit 3.4 S-N Diagram for Series B--Double Bolted Lap Splice: R = 0.

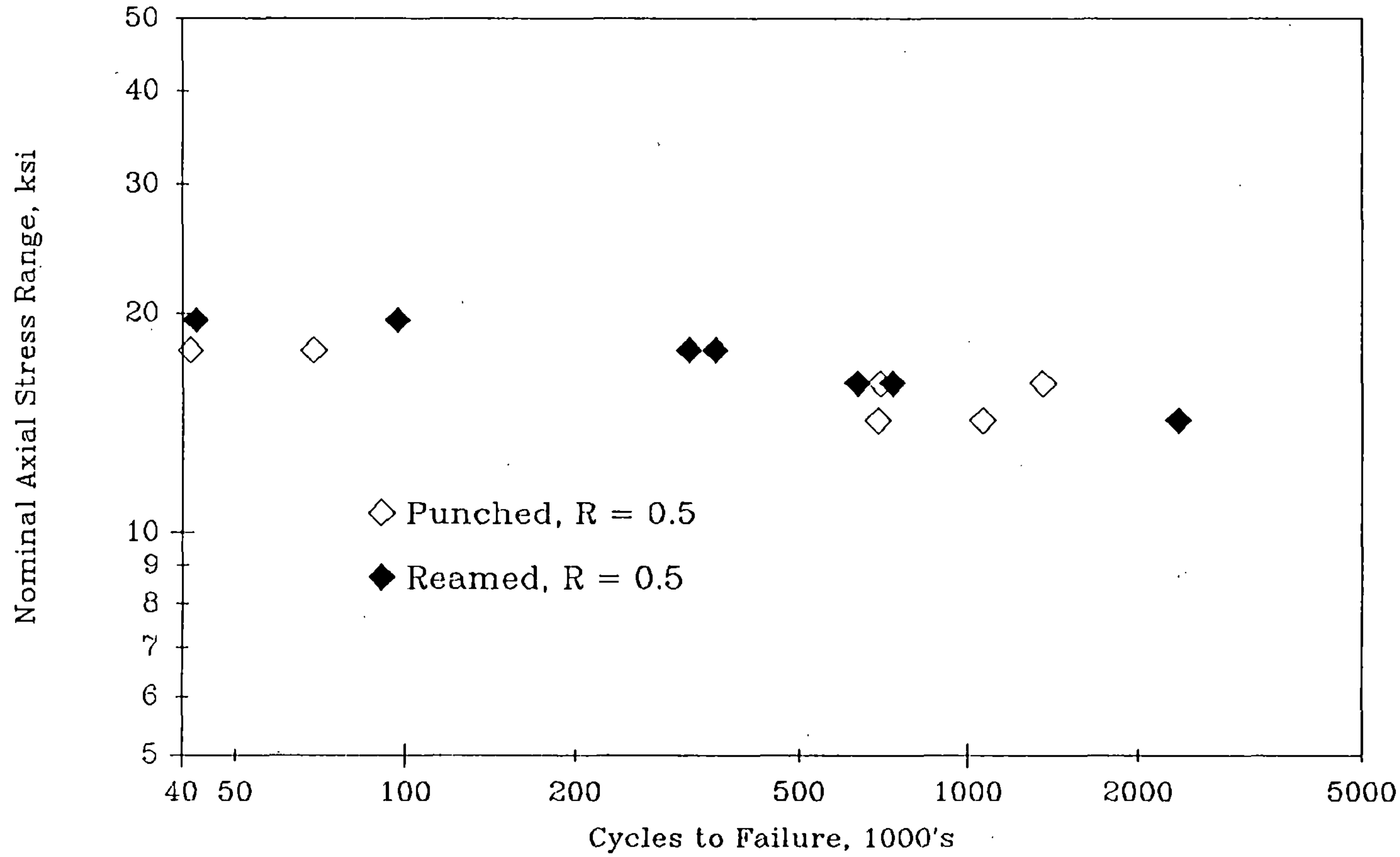

Exhibit 3.5 S-N Diagram for Series B--Double Bolted Lap Splice: R = 0.5.

in Exhibits 3.3, 3.4 and 3.5. For each series, four sets of results are presented: for R = 0 and 0.5, and two methods of hole preparation, namely punched and sub-punched and reamed. The results for Series B for R = 0.5, see Exhibit 3.5, are presented separately without regression analysis because of the uncertainty of the effect of the testing machine grips. The possibility of premature failure in the grips, combined with the apparent shallow slope of the S-N diagram, are of concern. Because it was not possible to test Series A and B for R = -1, Modified Goodman Diagrams (MGD) were not constructed.

3.4 COMMENTARY

For all data included in this section a failure through the net section occured. In the case of Series A this result was conclusive since there was only one net section which was critical and it was also subjected to flexural stresses produced by eccentricity of loading. However, for Series B instances of failure at the net section for one aluminum plate and at the grip for the other were observed. Recorded video monitoring of the process showed that first failure at the grips was a possible event for R= 0 tests. Such an event seemed to be more likely when small distortions in the aluminum plates resulted in a small but visible flexing of the plates in Series B under load. This problem could have been avoided by having a greater ratio of gross width at the grips to net width at the failure section. The 1.26 used for these tests fails to meet the ratio of 1.5 used in tests reported in the literature.

4.0 FLEXURAL FATIGUE TESTS

4.1 GENERAL

Current design methodology requires the testing of essentially full scale structural elements to elicit the effects of geometry, residual stresses and imperfections arising from manufacture, load history and material type. To extend the available data on the fatigue behavior of fillet welded beams fabricated of aluminum, two series, G shown in Exhibit 4.1 and H shown in Exhibit 4.2, were manufactured for test. These series were models of the bolster beam and the use of bolted cover plate terminations, respectively.

4.2 TEST ARRANGEMENT

The flexural test program for both Series G and H used a beam span of 11 ft.- 6 in. and beam depth of approximately 12 in. With a symmetrical load placement of two loads at 1 ft spacing, a peak total load capacity of 100 kips was needed to obtain nominal flexural stresses of 40 ksi. The arrangement used to satisfy these requirements is sketched in Exhibit 4.3 and illustrated in the photograph in Exhibit 4.4.

Load application was made using a distributing beam, rollers and bearing blocks. A 110 kip capacity MTS actuator and associated servo-control system were used for each frame. The loading rate was limited to a range of 0.75 step 1 Hz. because of the larger displacements characteristic of aluminum

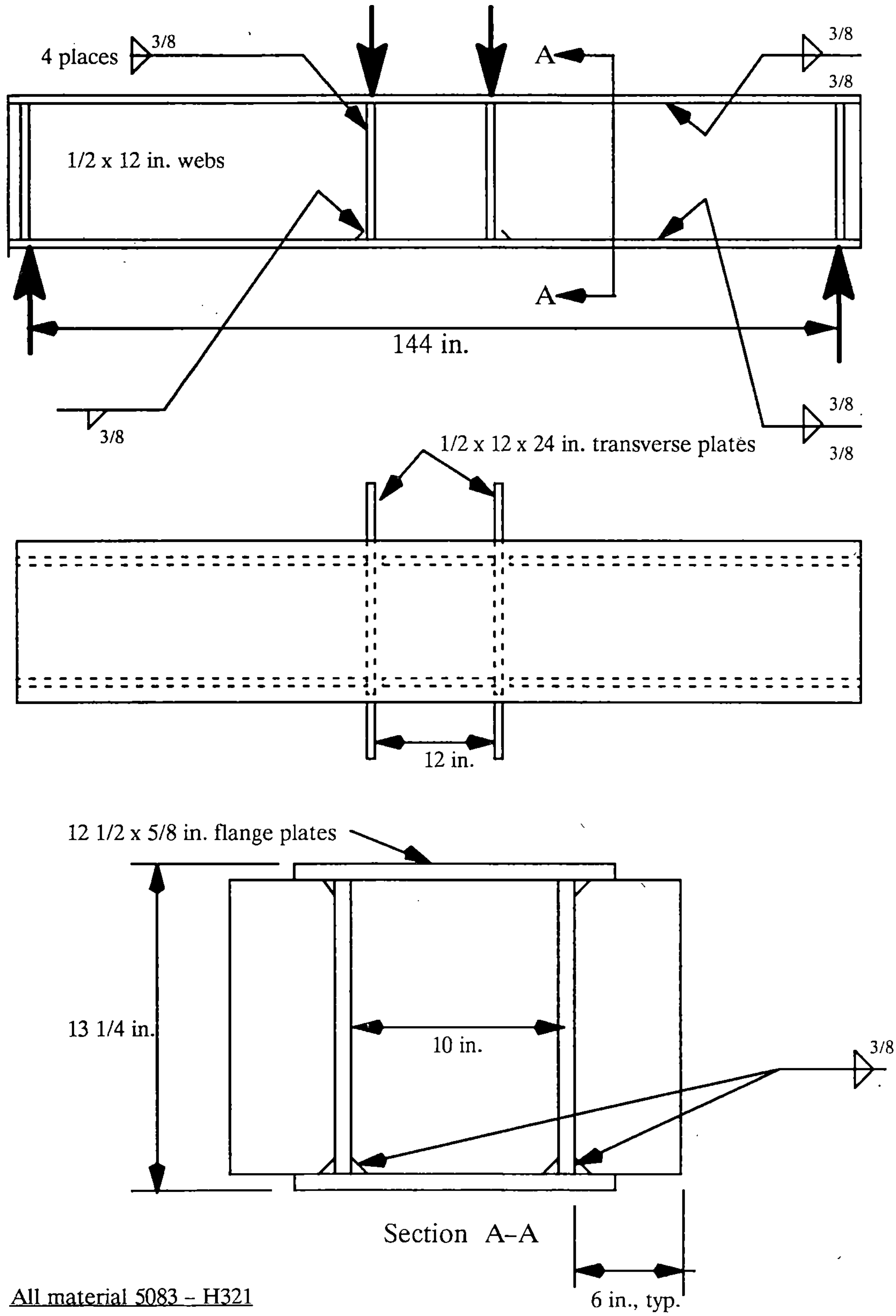

Exhibit 4.1 Welded Box Beam Simulating a Car Body Bolster--Series G.

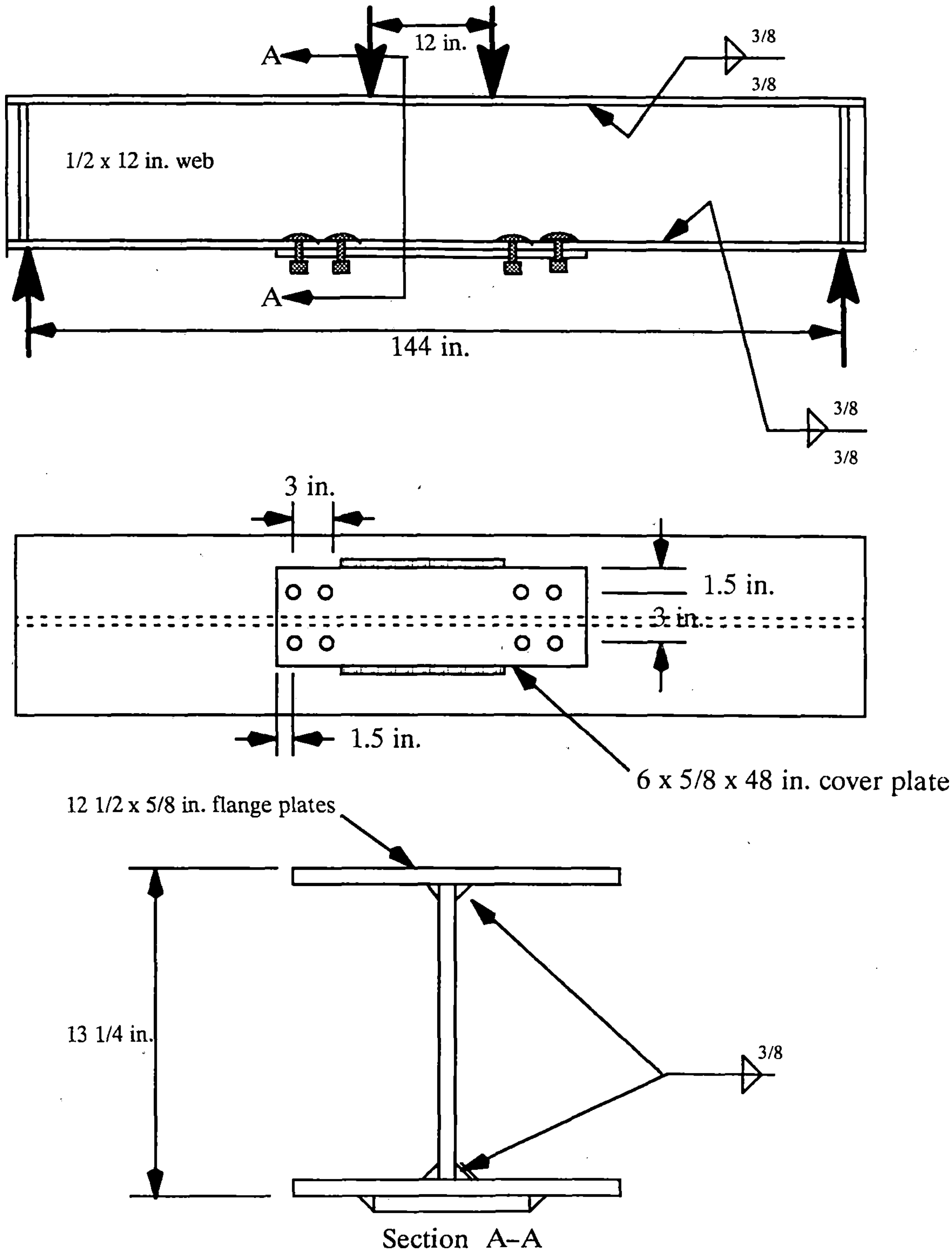

All material 5083 - H321

Exhibit 4.2 Welded I-Beam with Cover Plate using Bolted Termination--Series H.

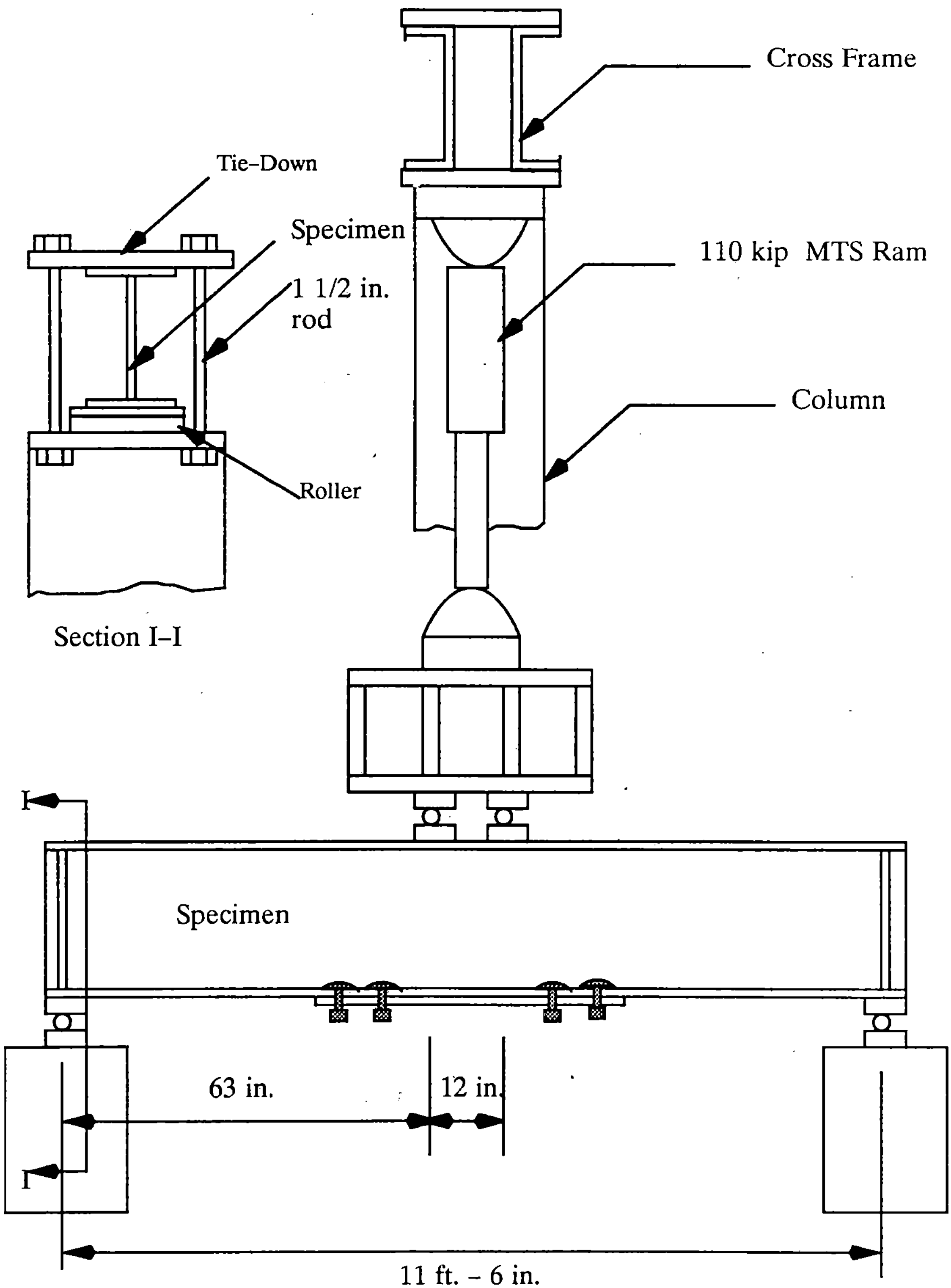

Exhibit 4.3 Sketch of Apparatus for Beam Tests on Series G and H.

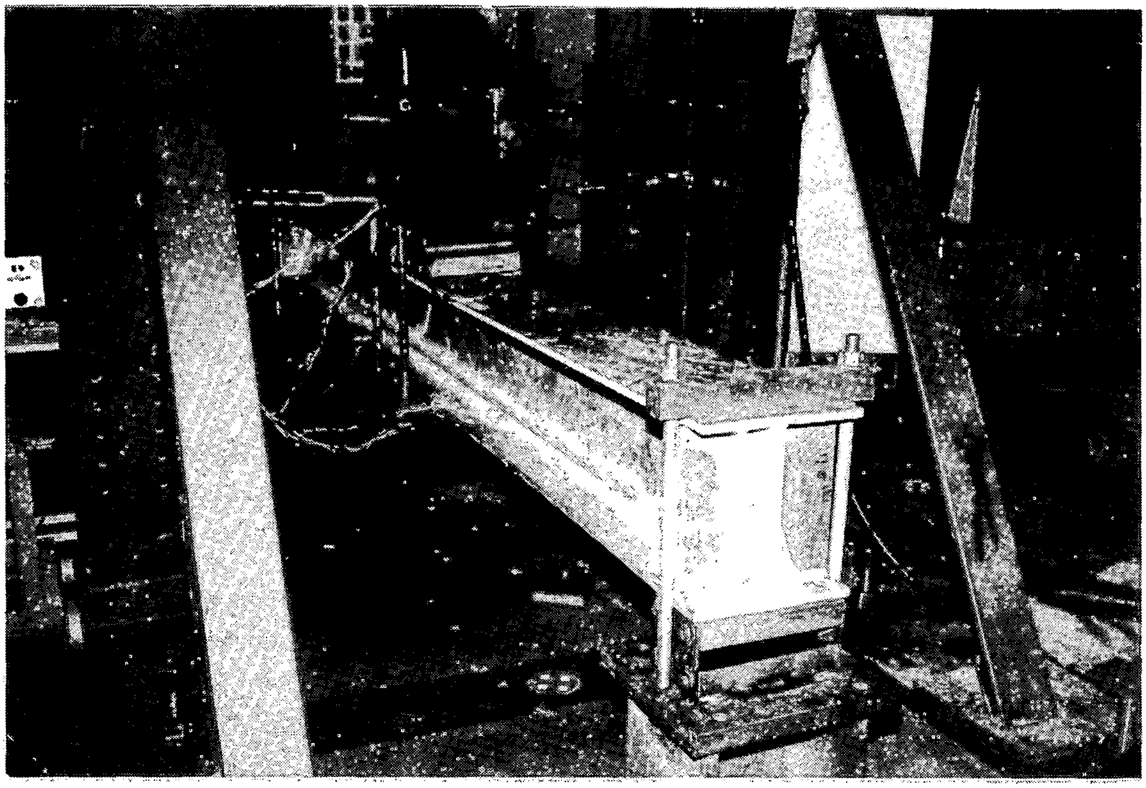

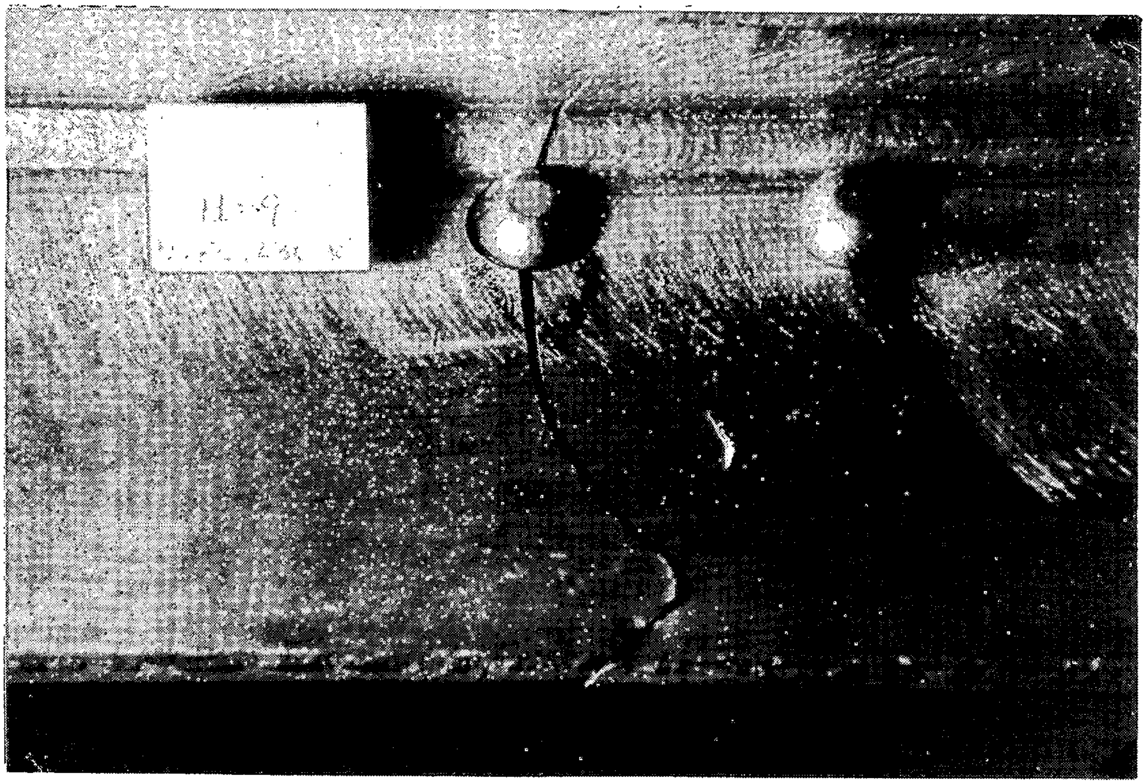

Exhibit 4.4 Photographs of Series H Test.

construction.

The supports and load application details consisted of a 2 in. diameter, 11 in. long roller, resting on a bearing plate with a 7 in. radius concave surface and a flat bearing plate on the top. Side plates were attached to the bearing plates with loose fitting bolts to act as keepers to prevent lateral drift of the rollers. For all tests, tie rods were used to maintain compression across the roller assembly, clamp the bearing plates to the beam flanges and to aid in initial alignment of the specimen.

All beam specimens were instrumented with strain gages to give a confirmation of the nominal moment or flexural stress level at midspan. In the G Series, strain gages were placed at selected locations near the fillet welds. At the start of the beam test program, gages were placed to give both top and bottom flange strains. To simplify and speed the testing after experience was gained with the nature of the static strains to be expected, the strain gage instrumentation was simplified to four gages on the bottom flange only. In all instances, deflections were measured at one point at midspan.

The standard test procedure was to take strain readings and deflection measurements at least four increments up to the intended maximum load for the fatigue test. These measurements define the static response during the "set-up" cycle and in all cases represent the first time that the specimen carried on applied load. In almost all cases, these measurements indicated indirectly the presence of residual tensile stresses in the fillet welds, because of small or moderate non-linearities in both strains and deflections in the first quarter-cycle of loading. The load was returned to zero and then cycled back to the test maximum and then to zero again. The second loading cycle invariably showed linear behavior in both strains and deflections.

Following the set-up cycle measurements, the fatigue testing was started. Strains were monitored on a peak-reading meter but were not recorded during the test. The tabulated stress levels are those corresponding to the nominal calculated stress corresponding to the test peak load. In general, there was good agreement between the nominal stress and measured strains, considering that only four strain measurements across the section were taken and that there was some influence of residual stresses and distortional stresses.

4.3 PRESENTATION OF DATA

The S-N data are presented in Tables 4.1 and 4.2 and in Exhibits 4.5 and 4.6. The basic presentation of the results of the flexural tests is in the form of S-N Diagrams in the conventional form of log-log plots of stress range versus cycles to failure. All stresses are shown in ksi and represent nominal values of flexural stress at the critical section: at the point of interruption of the web in Series G and at the net section of the bolted cover plate connection, the outer line of holes. Linear regression analyses were run for all data sets and the results are summarized in Section 6.

Table 4.1 Test Results for Series G Box Beam with Interrupted Web Simulating Bolster Beam.

($2S_x$/(side span) = 3.6698 in.^{2})

Number	Load (kips)	Stress Range (ksi)	Cycles to Failure 1000's	Notes	Plot Symbol
1	85	23.16	145.00	R = 0	Open Triangle
2	40	10.90	166.60	R = 0	Open Triangle
3	40	10.90	577.20	R = 0	Open Triangle
4	70	19.07	639.70	R = 0	Open Triangle
5	27	7.36	1177.56	R = 0	Open Triangle
6	27	7.36	3870.56	R = 0	Open Triangle

Table 4.2 Test Results for Series H I-Beam with Bolted Cover Plate Terminations.

($2S_x$/(side span) = 4.35269 in.^{2})

Number	Load (kips)	Stress Range (ksi)	Cycles to Failure 1000's	Notes	Plot Symbol
1	40	9.19	671.50	R = 0	Open Triangle
2	40	9.19	929.30	R = 0	Open Triangle
3	80	18.38	81.20	R = 0	Open Triangle
4	75	17.23	104.72	R = 0	Open Triangle
5	30	6.89	1052.00	R = 0	Open Triangle
6	30	6.89	1498.00	R = 0	Open Square Failed at Midspan

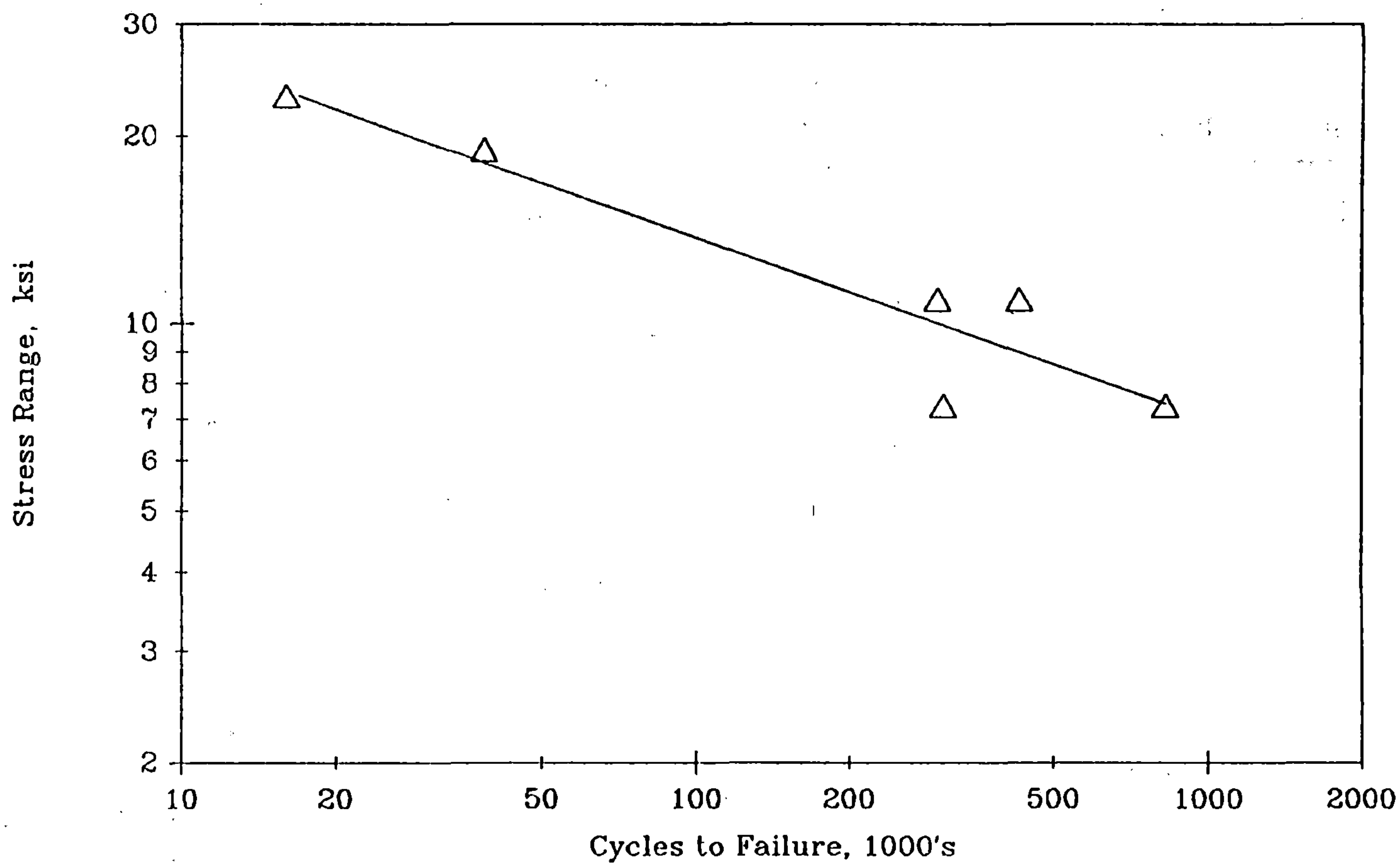

Exhibit 4.5 S-N Diagram for Series G--Box (Bolster) Beam with Interrupted Web.

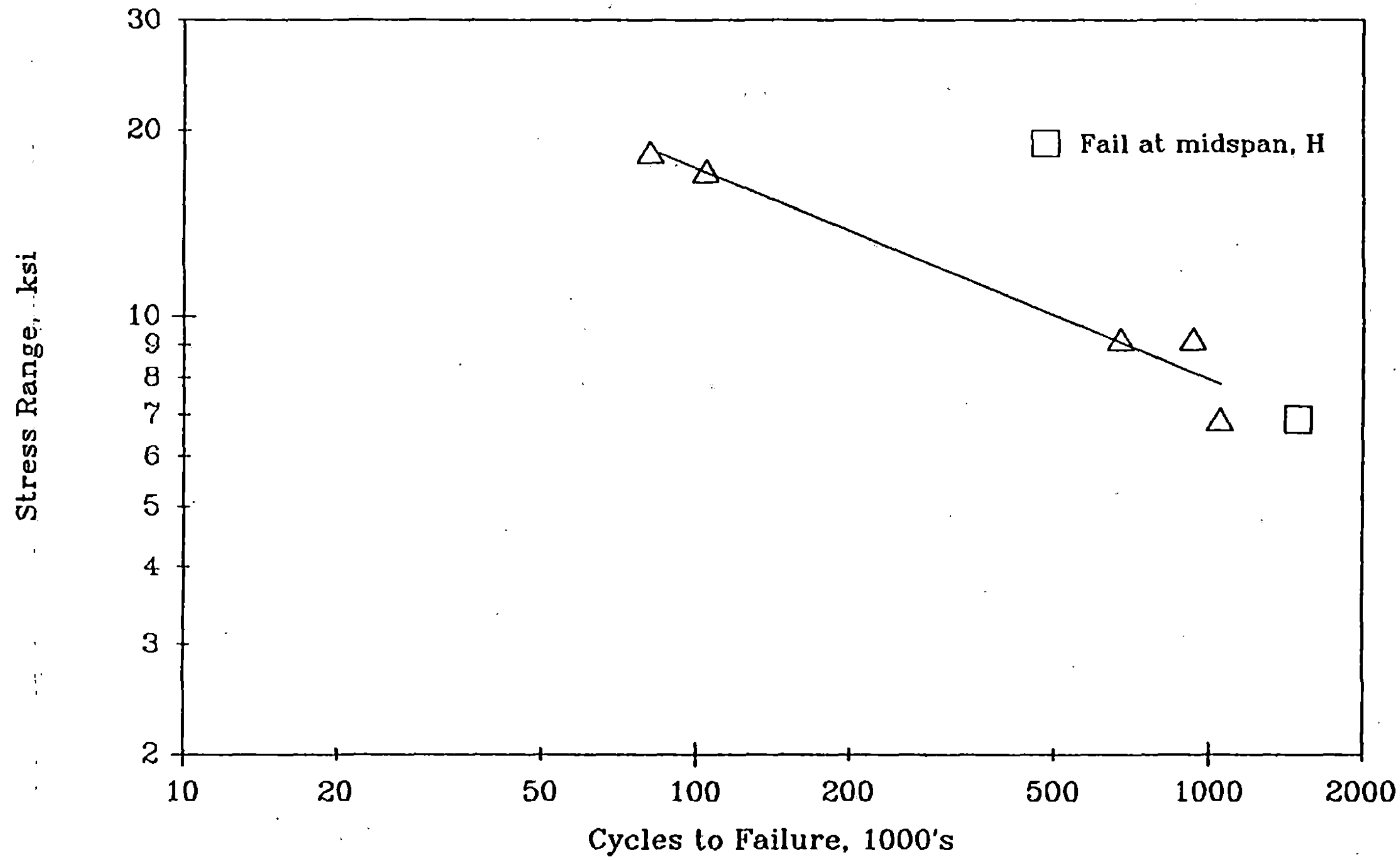

Exhibit 4.6 S-N Diagram for Series H--I-Beam with Coverplate and Bolted Termination.

4.4 COMMENTARY

Series G: These tests model the behavior of the bolster beam and are designed to simulate a car detail in a generic sense, although there is at least one design situation where this construction is used. The key to behavior, as was the case in the similar details tested in steel (see Ref.1), is the fact that the beam webs are interrupted by transverse plates at a point of essentially maximum bending moment. Fatigue cracking was found to initiate always in this region.

Series H: This series is designed to evaluate the use of bolted cover plate cut-off details. The critical section for fatigue failure is the net section through the outer row of bolt holes, i.e. where the coverplate stress carries no load and the full flexure is carried by the beam I-section alone. In one test, a fatigue crack developed at midspan and prevented the initiation of failure associated with the cover plate termination.

The flange plates of the I-section in Series H showed marked distortion due to the web-to-flange welds and careful shimming was required under the loading pads.

5.0 SPATE DEMONSTRATION TEST

During the test program, the decision to demonstrate the usefulness of the recently acquired "SPATE" (Stress Pattern Analysis by Thermographic Emission) unit of the Association of American Railroads was made. The following information on the SPATE unit is extracted from Reference 5 obtained from the manufacturer.

5.1 SPATE 9000 THEORY AND PRINCIPLE

The SPATE technique is based on the measurement of the thermoelastic effect, investigated by Lord Kelvin in 1853. Within the elastic range, a material subjected to tensile or compressive stress experiences a reversible conversion between mechanical and thermal energy causing it to change temperature. Provided that adiabatic conditions are maintained, the relationship between the change in the sum of the principal stresses and the corresponding change in temperature is linear and independent of loading frequency according to the equation

$$\theta = K_m \times T \times \sigma$$

where θ is the peak to peak temperature change,

K_m is the thermoelastic constant,

T is the mean temperature of the structure and

σ is the peak to peak change in the sum of the principal stresses. The thermoelastic constant of the material is expressed as

$$K_m = \frac{\alpha}{\rho \times C_\sigma}$$

where α is the coefficient of linear thermal expansion,

ρ is the density and

C_σ is the coefficient of specific heat at constant stress.

Calibration can simply be carried out by referencing a strain gauge placed in a region of uniform stress in the scan area. Alternatively calibration can be determined theoretically by using known properties of the materials in the equation

$$\sigma = \frac{-\rho \times C_\sigma \times D \times V}{\alpha \times T \times e}$$

where V is the signal produced by SPATE,

D is the SPATE calibration factor (known for each instrument)and

e is the emissivity of the surface (efficiency of the emission of infrared radiation).

5.2 HOW SPATE 9000 WORKS

SPATE 9000 detects the minute temperature changes (to a sensitivity of 0.001°C) which arise when a structure is cyclically loaded. It then correlates the measured signal with a reference signal derived from the loading system to give output proportional to the stress induced. The scan unit contains infrared and visual channels which are focussed on the structure to collect thermal radiation and to identify simultaneously, points being scanned using an eyepiece or projected light spot. Data acquisition is under computer control and raster-like scans are produced.

An electronic data processing system correlates the stress-induced thermal fluctuations detected by the scan unit with the reference signal derived from the structure or the load system. The correlation rejects all signal frequency and phase components other than those caused by the loading system. Stress levels are digitized, stored and displayed in color.

5.3 SPATE 9000 SPECIFICATIONS

Maximum field of view	25°x25°
Measuring spot diameter	0.02" at 10" from scan unit and 0.04" at 30" from scan unit
Focus range	10" to ∞
Stress resolution	Typically 58 psi in aluminum, 145 psi in steel
Stress frequency range	0.5 to 20,000 Hz
Measurement grid density	Up to 255x255 points
Liquid nitrogen hold time	Up to 4 hours
Specimen temperature range	In principle, specimen temperature can be in excess of 1800°F depending on physical constants of material. Optical filters may be required to avoid damaging detector.
Equipment temperature range	41 to 104°F
Power requirements	110 V rms, 5 A; 240 V rms, 2.5

	A; nominal 50-60 Hz
Console-only dimensions	35"x22"x28"
Scan unit dimensions	16"x13"x12"
Weight	Console: 163 lb excluding computer unit Scan unit: 55 lb

5.4 SPATE DEMONSTRATION

The 'Series-G' specimen-"Welded I-beam with cover plate using bolted termination" was selected for this purpose. A sketch of the specimen is shown in Exhibit 4.2. The specimen was placed in the test frame such that the loading produced tension on the flange with the cover plate, as shown in Exhibit 4.3. Exhibit 5.1 is a photograph of the actual setup showing the SPATE camera unit aimed at the bottom flange through a mirror placed on the floor underneath the specimen.

Exhibit 5.2 shows one of the SPATE scans. This scan was obtained by applying a cyclic loading at 10 Hz. The length of the scan area was 5" near the termination of the cover plate. The cover plate, which is 3" wide, is marked and also shown are the four Huck bolts. The color-coded scale of the stresses is shown on the right side of the scan. The observations were made by an examination of the scan 1. The Huck bolts near the end of the cover plate (two on the right side, in Exhibit 5.2) carry very negligible load, evidenced by the low stresses (200-600 psi) in their vicinity. It can also be seen that the cover plate itself in this region (near its end) is carrying a very small load.

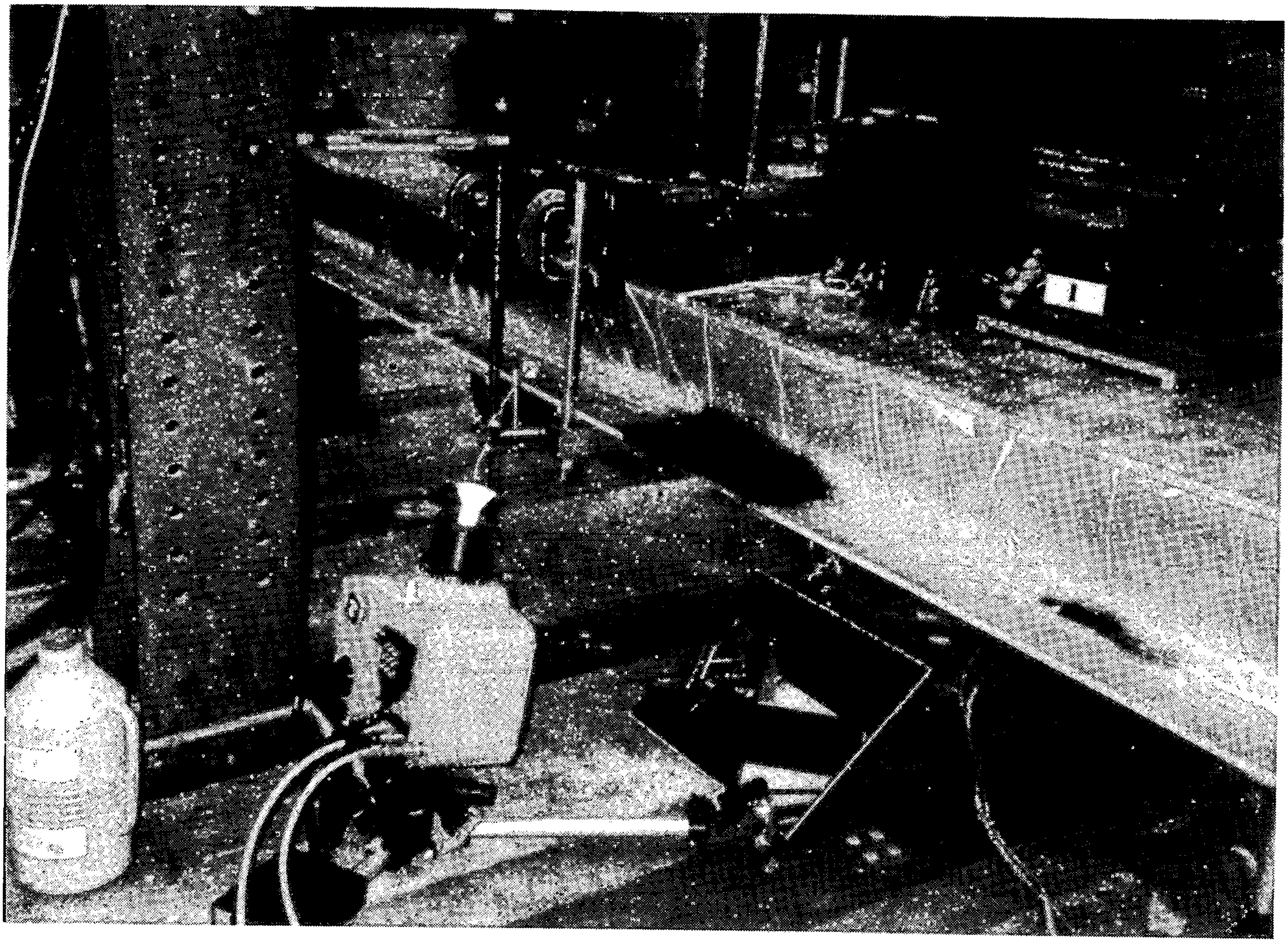

Exhibit 5.1 Photograph of the SPATE set-up

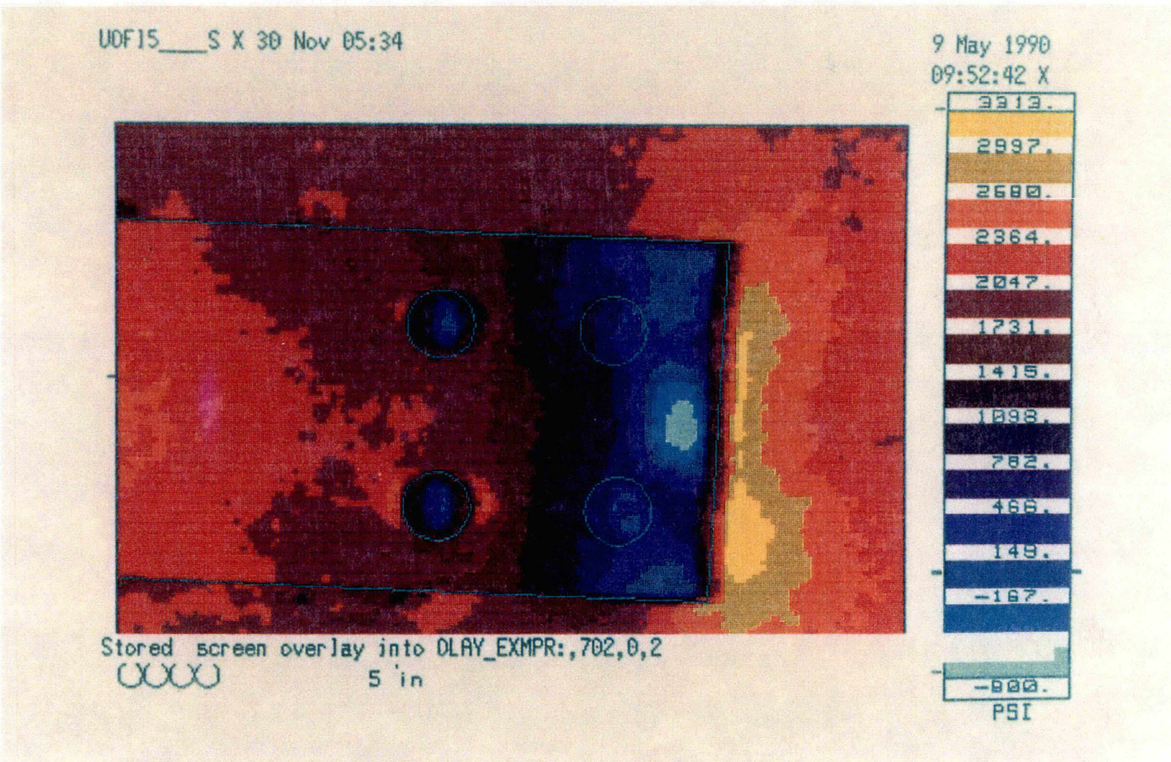

Exhibit 5.2 SPATE scan of Welded I-Beam with Cover Plate using Bolted Termination

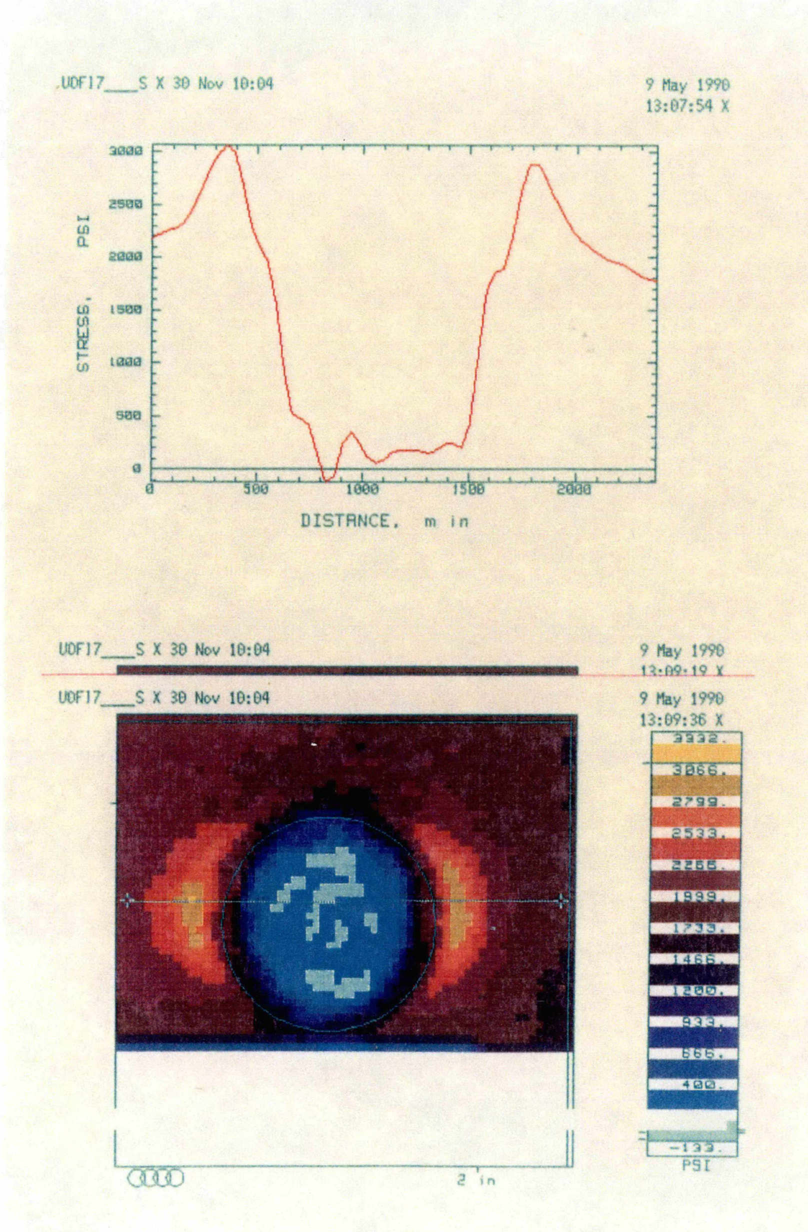

Exhibit 5.3 SPATE scan of the region around the Interior Huck Bolts

2. The stresses increase as one proceeds towards the two left side Huck bolts (these are closer to the center of the beam) and these Huck bolts are primarily transferring the load between the cover plate and the flange.

3. Just outside the cover plate, (just right of the cover plate end in Exhibit 5.2), the loading is carried fully by the flange only, as evidenced by a higher stress region (yellow color-3.3 ksi). Also the stresses decrease as one proceeds to the right (away from the center of the beam specimen).

4. At location 'A' of the exhibit, a local region of slightly higher stress than its surroundings can be seen. It was discovered that this is the region where one of the welds terminated. A finer scan of this area was done later (not shown here) and it was found that the stress concentration factor of 1.8 existed at the weld termination.

5. The region around the interior Huck bolts (location 'B') also displayed some locally high stress. Another scan was initiated wherein only the 2" region around the Huck bolt was scanned. This scan is shown in Exhibit 5.3. The region of stress concentration can clearly be seen. Also shown in Fig. 5.3 is a graph of the stresses along the cross-section through the Huck bolt. It was found that the stress concentration factor was approximately 2.0 near the Huck bolt.

6.0 SUMMARY AND RECOMMENDATIONS

6.1 SUMMARY

Fatigue tests on eleven different connection details in aluminum have been conducted and the results presented in tabular form and in S-N diagrams. A total of 119 fatigue tests were conducted. Commentary and discussion was presented for each test series and have indicated that the behavior of all test series was within expectations for the detail geometries tested.

The data describing all S-N diagrams presented in this study are summarized in Table 6.1. The regression coefficients (LogS = A0 - A1 LogN), parameters for fatigue life determination, C and m (Life, $N = C/S^m$), and the projected fatigue strengths associated with lives of 100,000 and 2,000,000 cycles are contained in the tabulation. The quantities S_{100} and S_{2000} denote the stress ranges in ksi corresponding to lives of 100,000 and 2,000,000 cycles, respectively.

With one exception the correlation coefficients are characteristically high, often above 0.95, denoting the suitability of the logarithmic plot of the S-N diagram and the use of a simple power law to relate stress range and fatigue life.

Table 6.1 Regression Matrix for Tests Conducted.

Detail	R	A0	A1	Corre-lation, ρ	C	m	S_{100} (ksi)	S_{2000} (ksi)
A,1 (Punched)	0	1.4452	0.15691	0.96187	1.62E+09	6.373	13.53	8.46
A,2 (Reamed)	0	1.5396	0.20015	0.96829	4.92E+07	4.996	13.78	7.57
A,3 (Reamed)	0.5	1.6692	0.30261	0.95796	3.28E+05	3.305	11.59	4.68
A,4 (Punched)	0.5	1.5264	0.24268	0.95351	1.95E+06	4.121	10.99	5.31
B,1 (Punched)	0	1.7529	0.18875	0.91023	1.94E+09	5.298	23.74	13.48
B,2 (Reamed)	0	2.1184	0.31283	0.95801	5.91E+06	3.197	31.10	12.18
B,3 (Reamed)	0.5	1.4483	0.08445	See text				
B,4 (Punched)	0.5	1.3271	0.04684	See text				
C	0	2.0946	0.42679	0.87331	8.09E+04	2.343	17.42	4.85
D	0	1.2935	0.20370	0.97352	2.24E+06	4.909	7.69	4.18
E	0	1.3973	0.25890	0.99189	2.49E+05	3.862	7.58	3.49
F	0	1.2382	0.20991	0.88968	7.92E+05	4.764	6.58	3.51
G	0	1.7217	0.29187	0.93742	7.92E+05	3.426	13.74	5.73
H	0	1.9190	0.33961	0.97904	4.47E+05	2.945	17.37	6.28
I	0	1.3174	0.27470	0.98994	6.25E+04	3.640	5.86	2.57
J	0	1.1520	0.25427	0.97320	3.39E+04	3.933	4.40	2.05
K	0	1.2794	0.29396	0.93930	2.25E+04	3.402	4.91	2.04

6.2 RECOMMENDATIONS FOR FUTURE RESEARCH

The volume of testing conducted over a wide variety of test configurations leads to the first recommendation that the test volume be expanded for the most important details used in car building practice. There are in addition, several phenomena which need additional investigations for completeness: (1) Expanded investigation of bolted connections to include such factors as bolt spacing (usually expressed relative to bolt diameter), the ratio of shear area to bearing area, and in the present configuration the influence of the mastic used in the joint; (2) The number of bolts needed for effective termination of cover plates and perhaps the use of adhesives in this application; and, (3) The influence of flexibility in the various lap splice configurations tested.

In connection with the program of expanded bolted joint investigation (item 1 above), a specimen design should be adopted which would readily allow full reversal tests. The data collected herein is intended to be used in applications with a linear damage rule, Miner's hypothesis, and is usually combined with an estimate of the variable history of fatigue loading experienced by the car. It is important to establish the degree to which this fatigue analysis procedure is reasonable for full scale flexural specimens with realistic details and a variable amplitude fatigue loading. Implied in such tests are both the definition of one or several fatigue loading histories (or stress blocks) and then a series of tests under variable amplitude loading.

7.0 REFERENCES

1. W. H. Walker, Walsh, W. J., and Lawrence, F.V., "Laboratory Fatigue Testing of Selected Welded Steel Connections for Freight Car Design," Report R-645, AAR Technical Center, 3140 South Federal Street, Chicago, Illinois September 1987.

2. F. Wattar, Albrecht, P., and Sahli, A., "End-Bolted Cover Plates", J. Structural Engineering, ASCE, Vol. 113, No.6, June 1985.

3. Pedro Albrecht, "Fatigue Strength of Adhesively Bonded Cover Plates", J. Structural Engineering, ASCE, Vol. 113, No. 6, June 1987.

4. J. D. Burk and Lawrence, F. V., "Effects of Lack-of-Penetration and Lack-of-fusion on the Fatigue Properties of 5083 Aluminum Alloy Welds", <u>Welding Research Council Bulletin</u>, No. 264, ISSN 0043-2326, Welding Research Council, New York, NY, January 1978.

5. SPATE 9000 Dynamic Stress Analysis-OMETRON Inc., 44873 Falcon Place, Sterling, VA 22170

APPENDIX A

PHOTOGRAPHS

A.1 General

The photographs presented herein illustrate the nature of the failures characteristic of the various test series. In the following sections a brief textural description is provided to introduce each series of photographs.

A.2 Series A

All fractures occurred at the net section. Figs. A1 and A2 shown the failure section location and the failure surface.

A.3 Series B

The fracture surfaces shown in Figs. A3 and A4 are for the net section with both plates failing at the net section. The alternate failure pattern consisted of failure in a similar appearance at the net section in one plate and failure of the other plate in the testing machine grip.

A.4 Series C

In Figs. A5 and A6 the fracture location and fracture surfaces are shown. Failure occurs in both of the weld zones.

A.5 Series D

In Figs. A7 and A8 the fracture location and fracture surfaces are shown. Failure occurs in the weld.

A.6 Series E

In Fig. A9 the fracture surface is shown, including the region of partial penetration in the butt weld.

A.7 Series F

In Fig. A10 the fillet weld detail connecting the tube to the attachment pad is shown. The fatigue crack appears as a dark line at the toe of the fillet and extends around about one-third of the circumference.

A.8 Series G

The bottom surface of the bottom flange with the crack penetrating well across the flange is shown in Fig. A11. In Fig. A12 the top surface of the flange in the region of the junction with the web plates is shown to illustrate the progress of crack growth up the connection toward the neutral axis of the beam.

A.9 Series H

In Fig. A13 the bottom surface of the bottom flange is shown illustrating the crack emerging from under the coverplate at the net section of the bolted termination. The top surface of the bottom flange is shown in Fig. A14 and shows the crack propagated across the flange from outer edge to the bolt hole, from there to the web-to-flange weld and then up into the web.

A.10 Series I

The failure zone in shown in Figs. A15 and A16, with views of both sides of the specimen presented. The crack surface passes along the toe of the intermittent welds of the lap splice and penetrated through the plate.

A.11 Series J

In Figs. A17 and A18 the specimen is shown with both segments fitted together and with the fracture surfaces visible. The fracture initiates at the outer face of the slot weld and propagates toward the outer edges of the plate.

A.12 Series K

The fracture across the wide plate of the splice is shown in Fig. A19; the shape of the fracture path shown the influence of both the side fillet welds and the central slot weld. In Fig, A20 the obverse side is shown to illustrate that the slot weld and the plate containing it are intact.

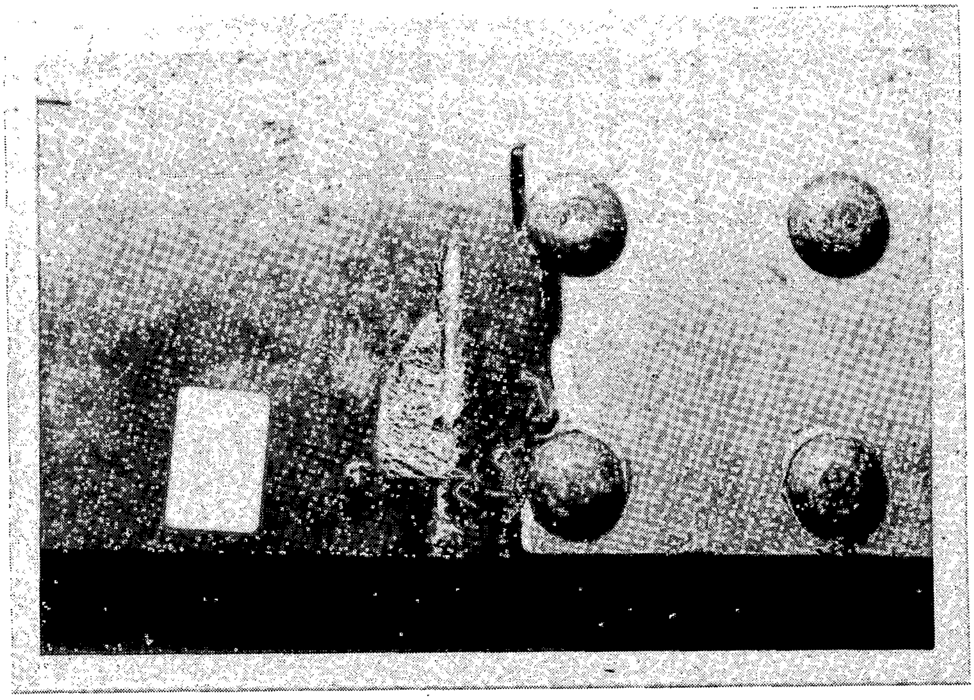

Fig. A1 Series A Showing Location of Fracture Path Across Net Section

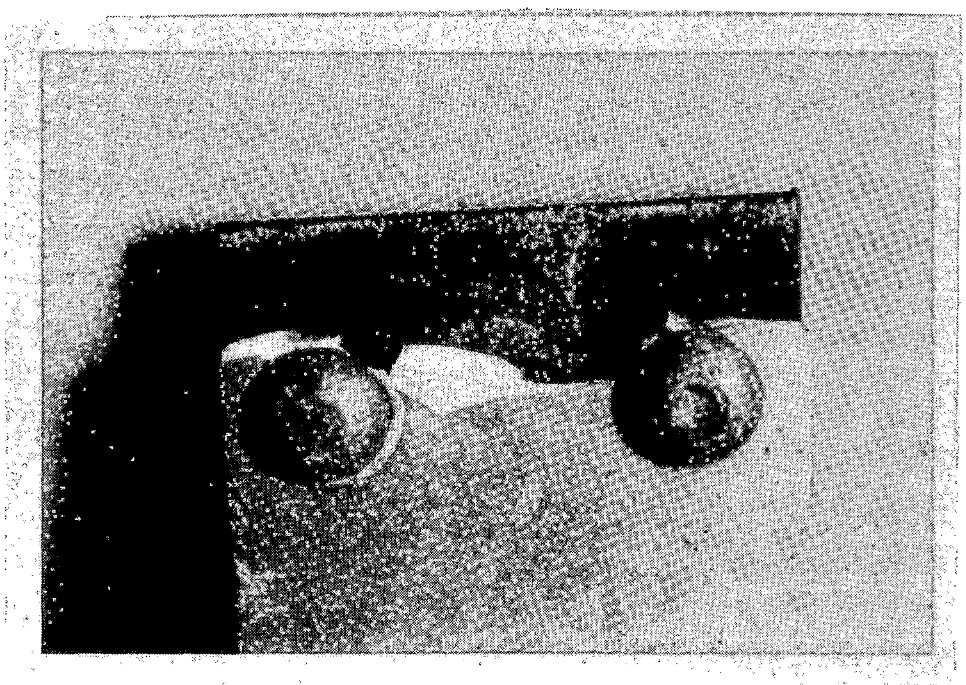

Fig. A2 Series A Showing Fracture Surface on Net Section

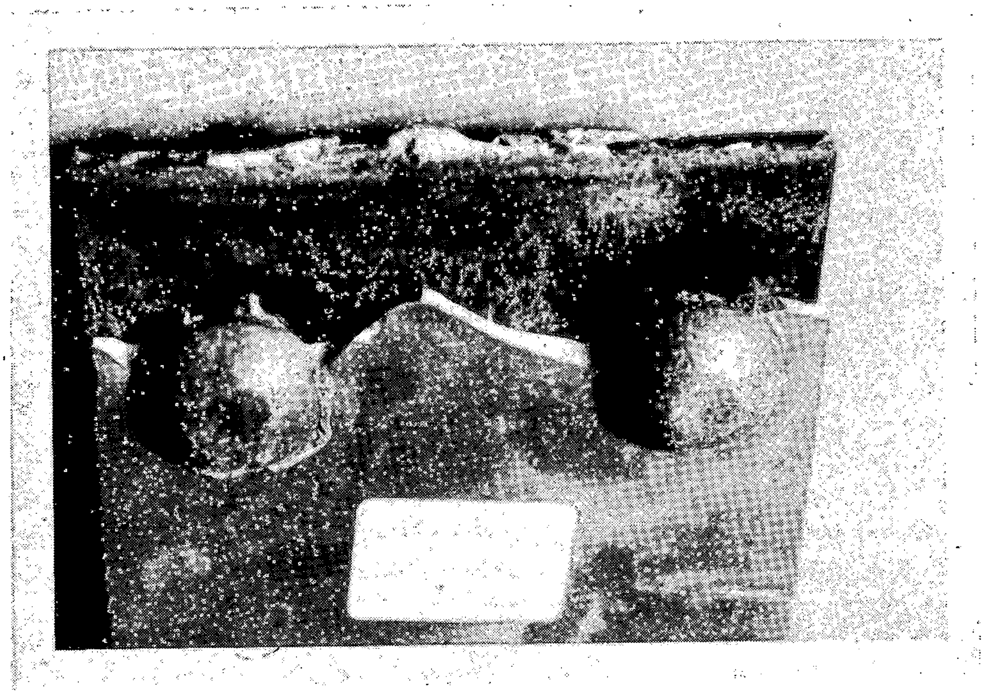

Fig. A3 Series B Showing Fracture Surface for Plate Adjacent to Bott Heads

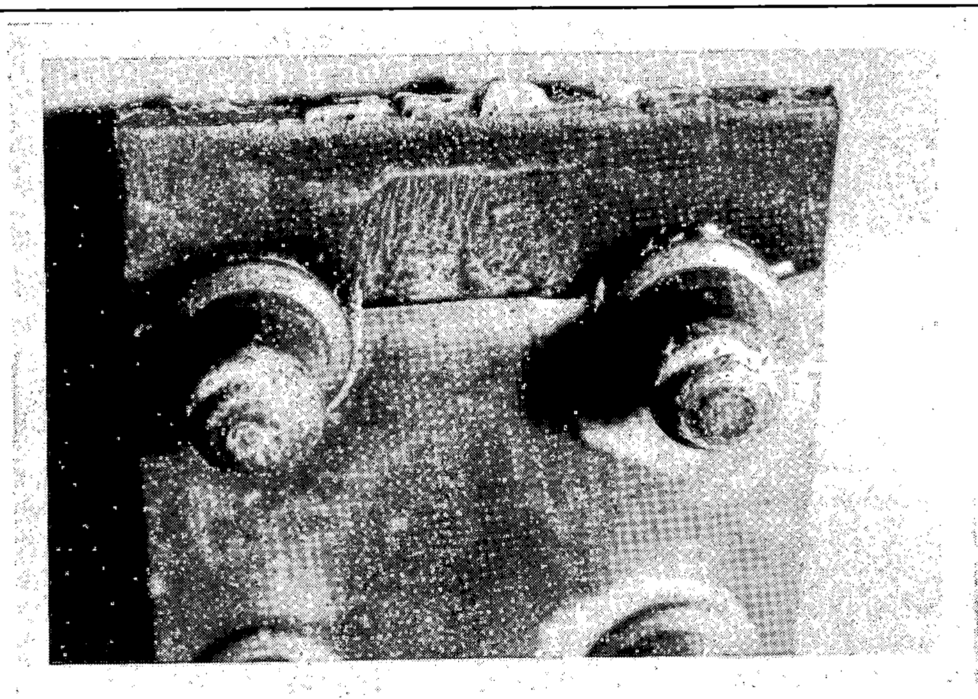

Fig. A4 Series B Showing Fracture Surface on Plate Opposite to Bolt Heads

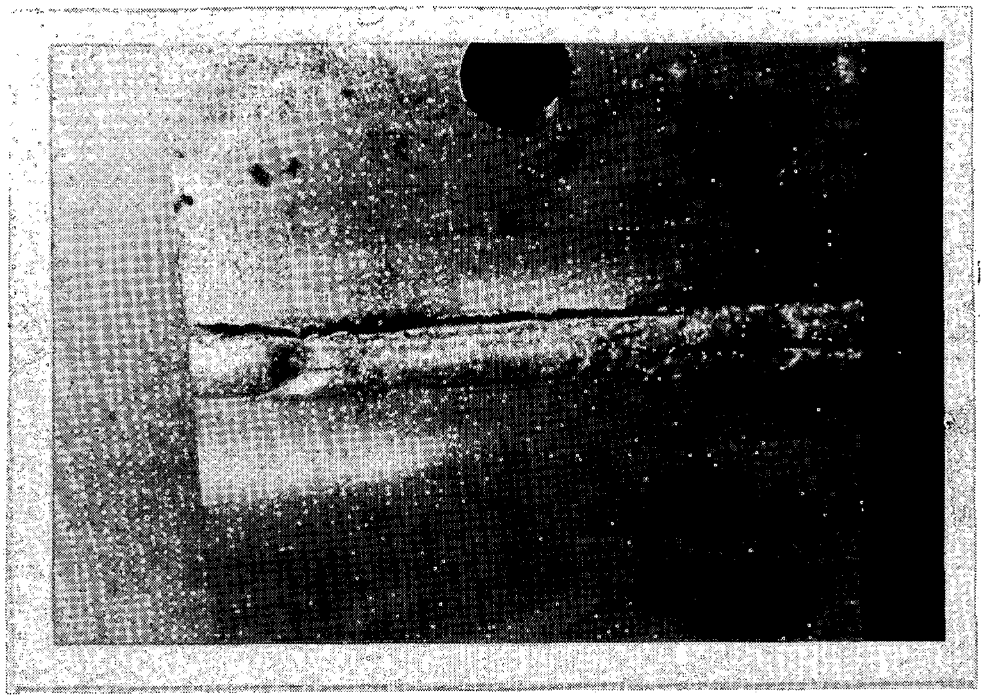

Fig. A5 Series C Showing Location of Fracture

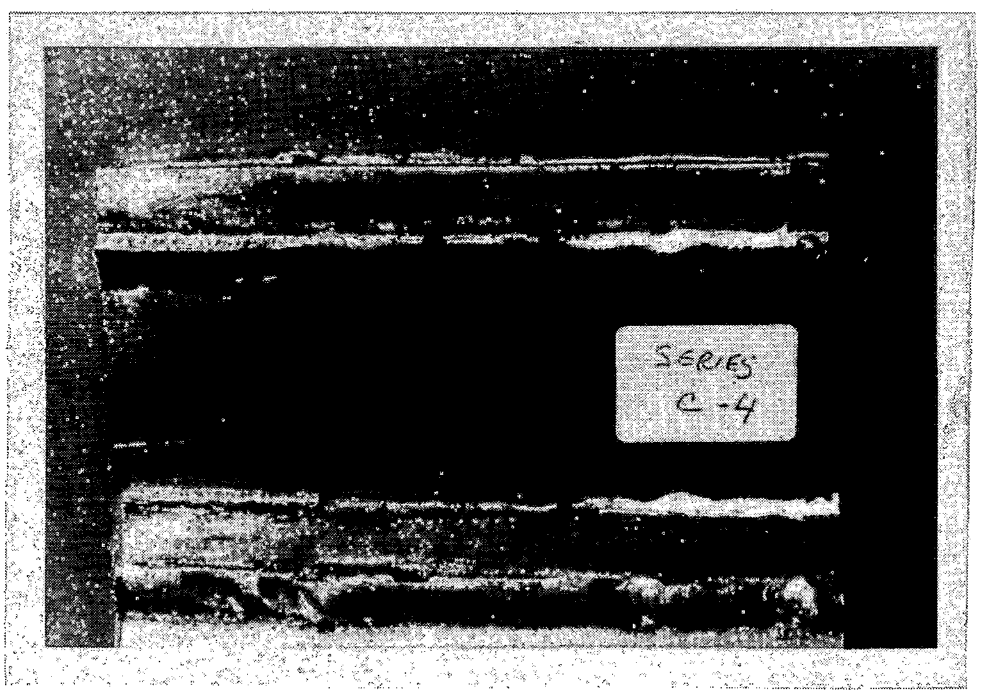

Fig. A6 Fracture Surfaces for Series C

Fig. A7 Series D Showing Fracture Location

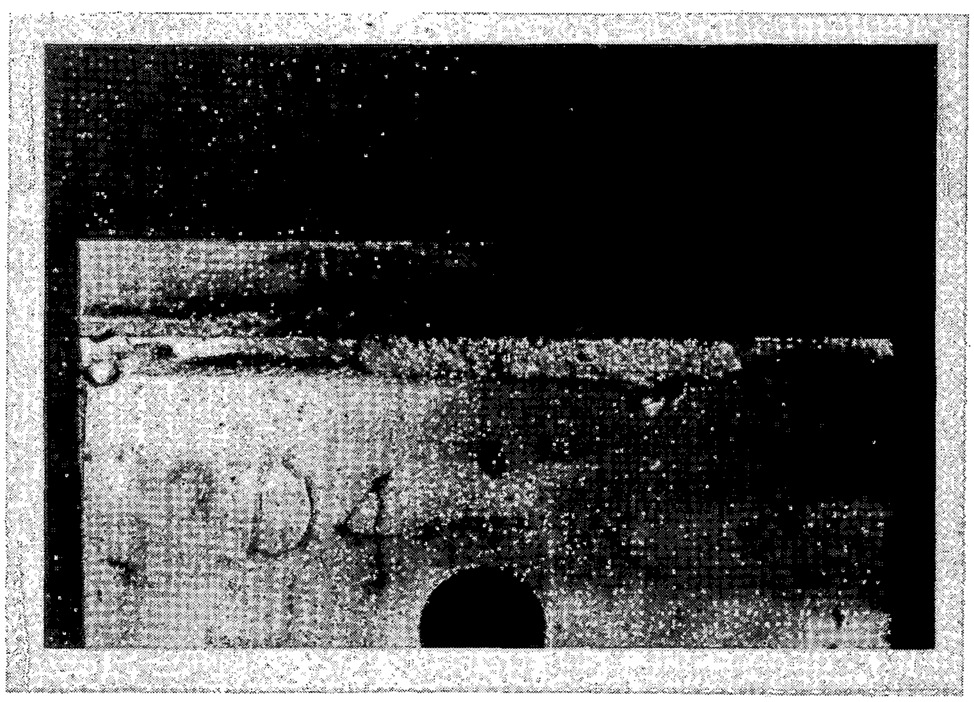

Fig. A8 Fracture Surface for Series D

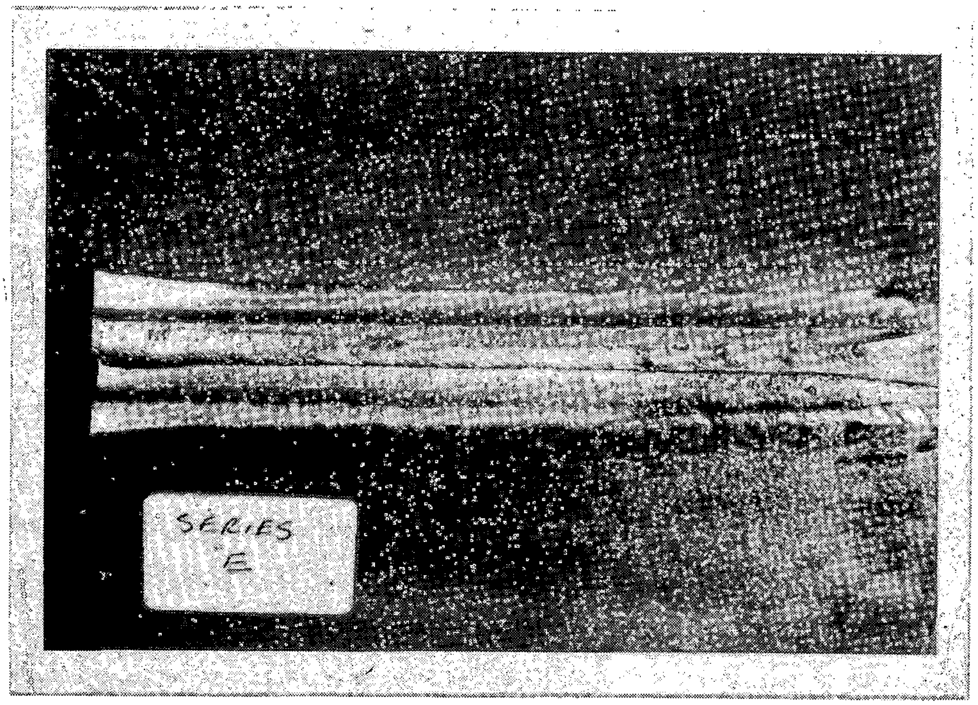

Fig. A9 Series E Showing Fracture Surfaces for Partial Penetration Butt Weld

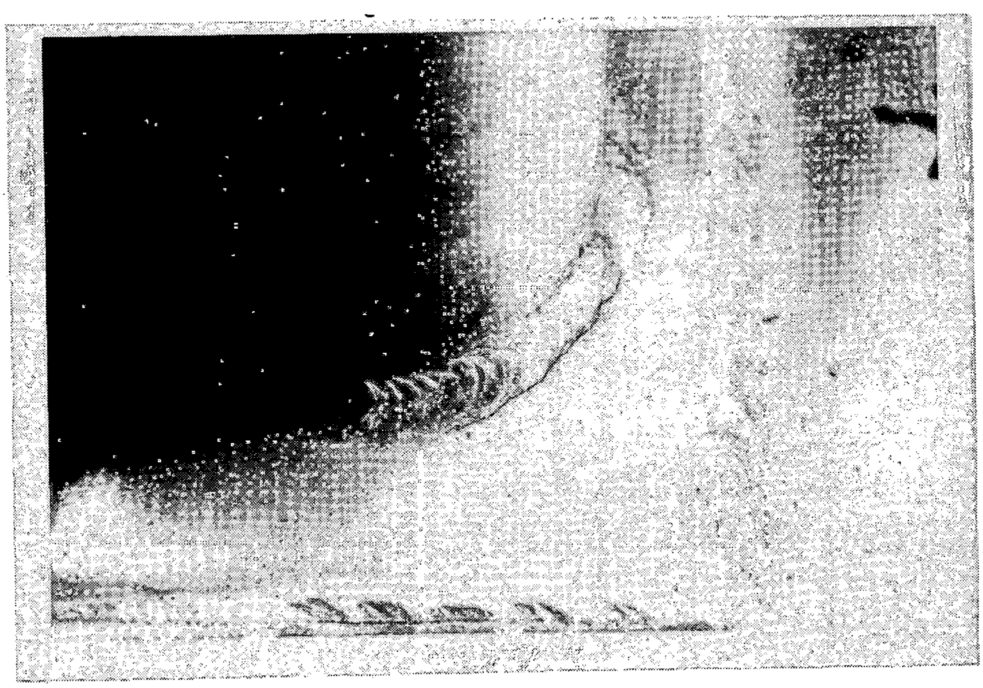

Fig. A10 Series F Showing Fatigue Crack at Fillet Weld Toe

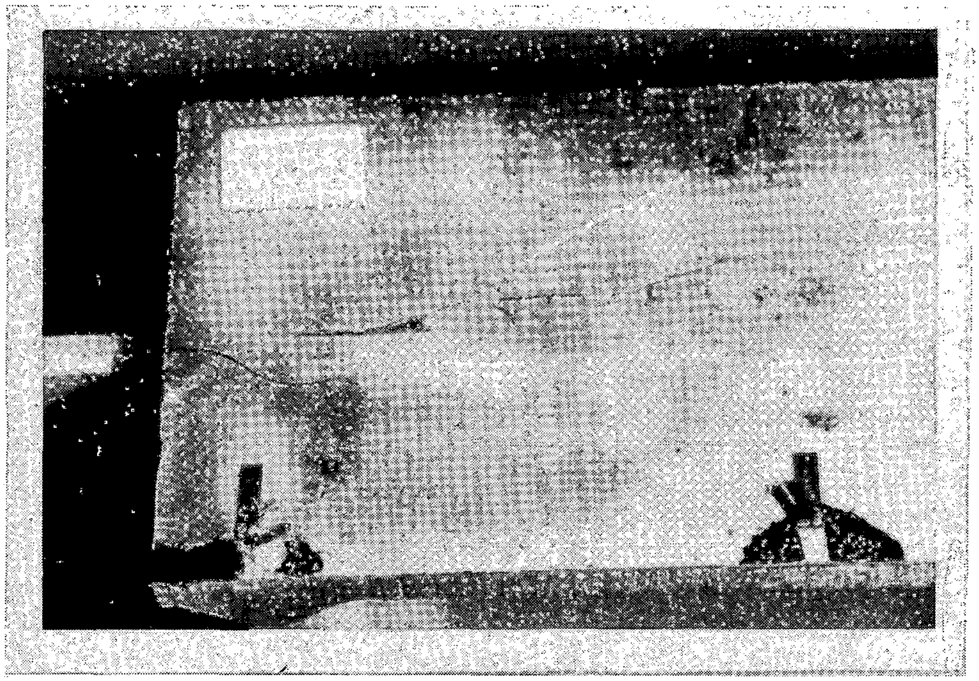

Fig. A11 Series G Box Beam Showing Crack Propagation Across Bottom Surface of Bottom Flange

Fig. A12 Series G Showing Crack Penetration into Web and Fillet Welds

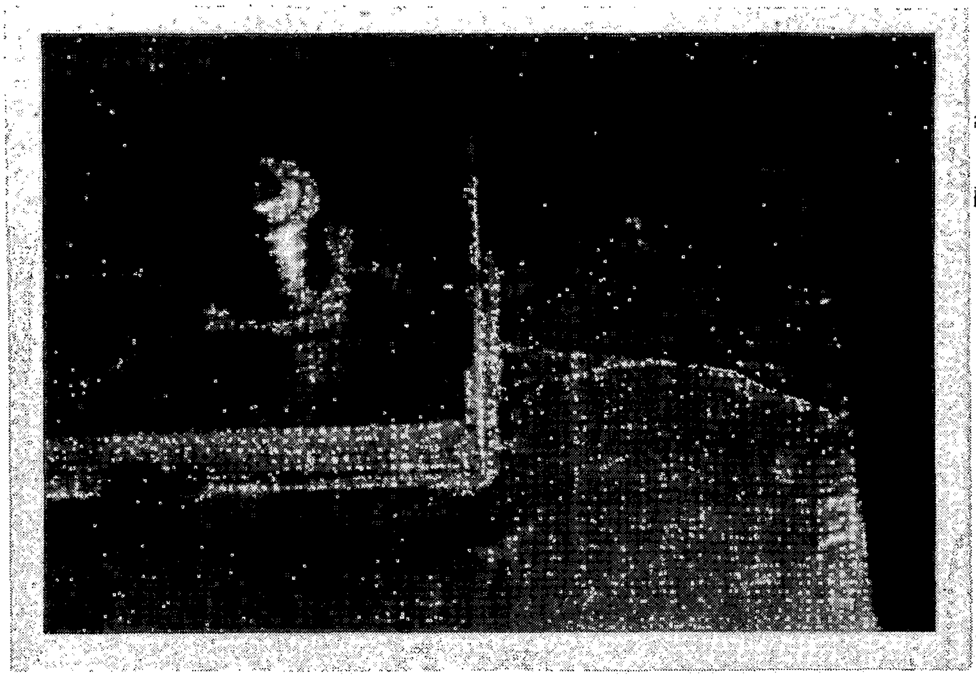

Fig. A13 Series H Bottom Flange and Coverplate Showing Crack Path Across Flange to Edge

Fig. A14 Series H Showing Top Surface of Bottom Flange and Crack Growth into the Fillet Weld and Web

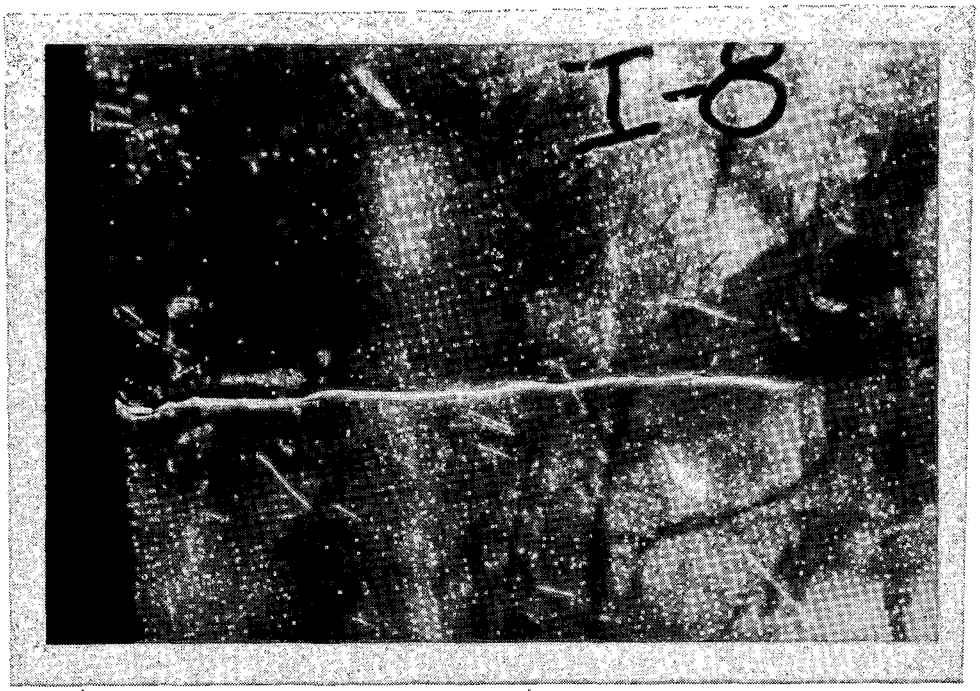

Fig. A15 Series I Showing Plate Side of Lap Splice

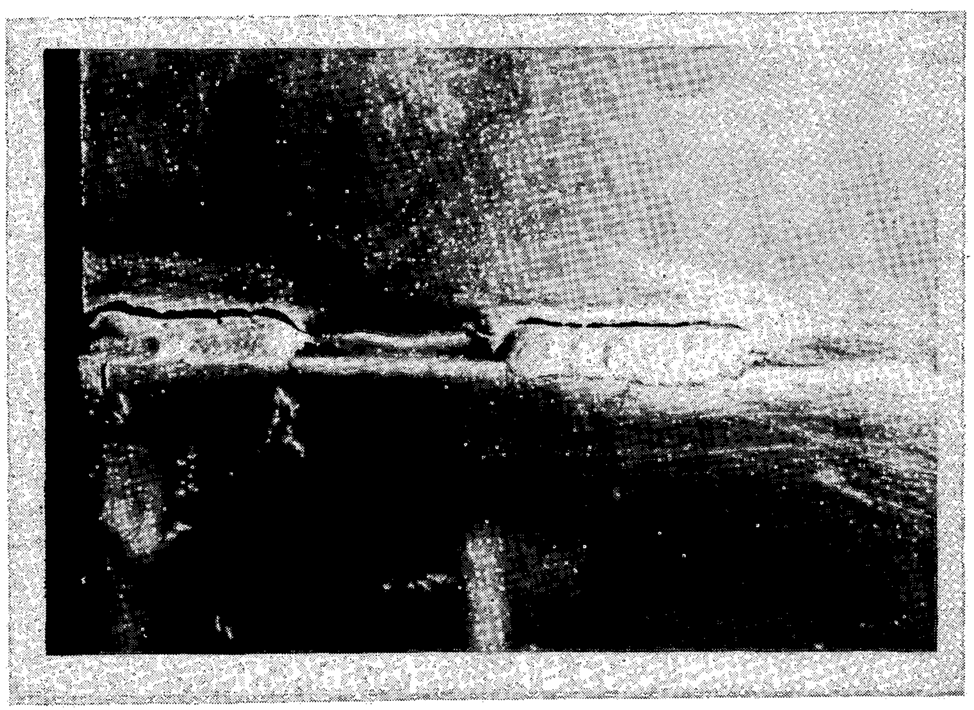

Fig. A16 Series I Showing Intermittent Welds and Crack Path

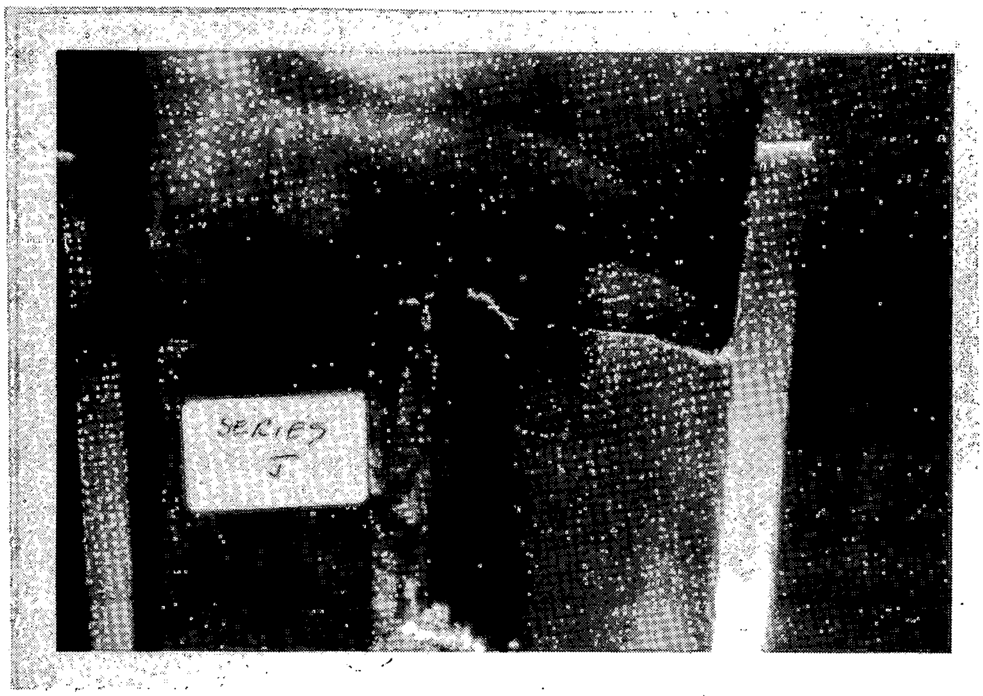

Fig. A17 Series J Showing Crack Path Across Plate Above Slot

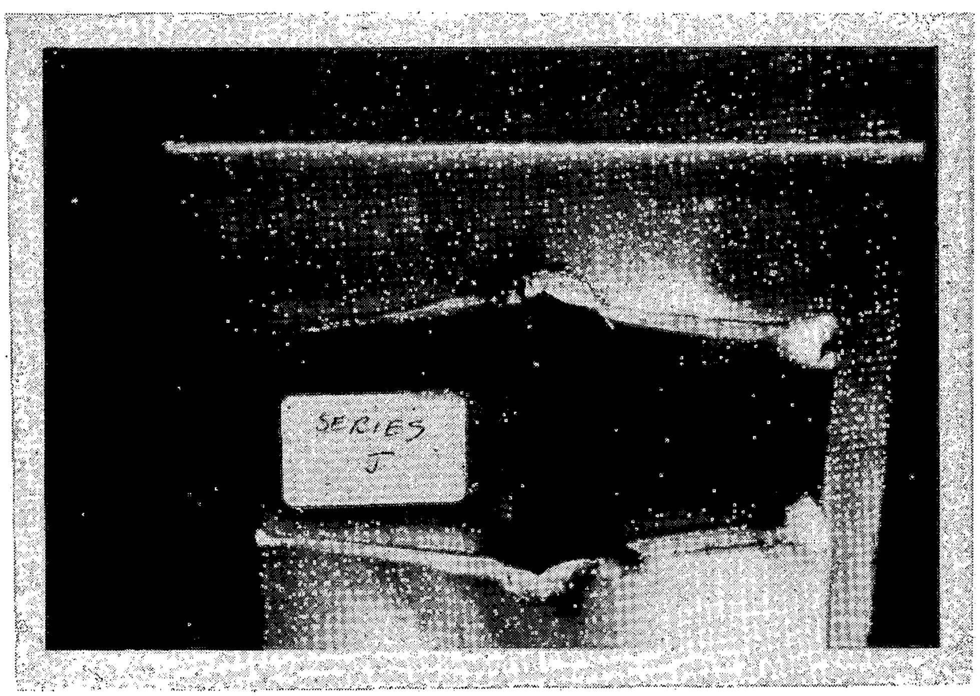

Fig. A18 Series J Showing Both Crack Surfaces

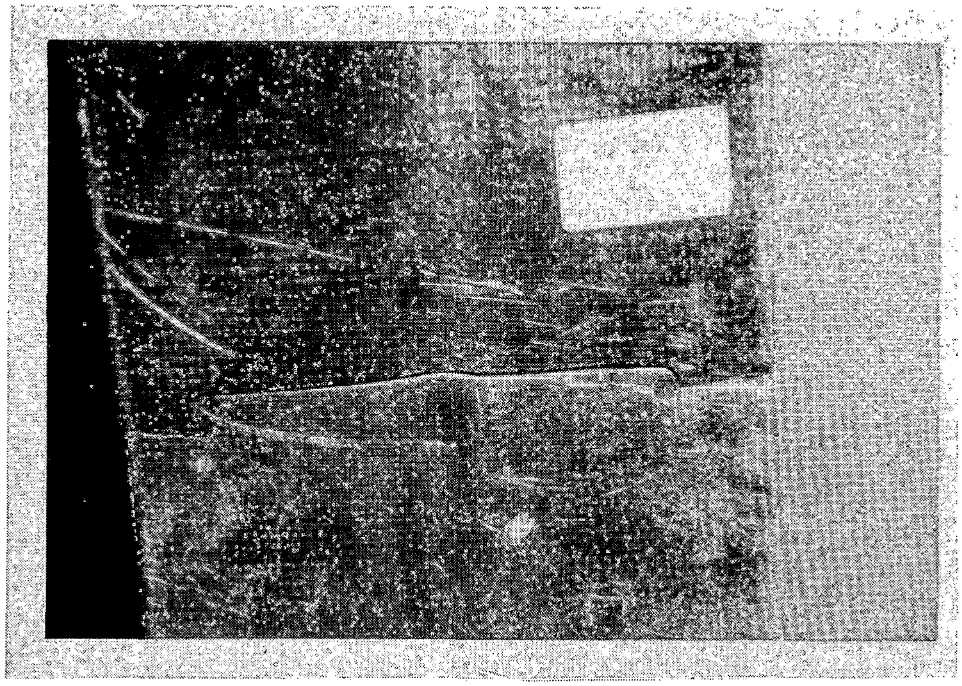

Fig. A19 Series K Showing Crack Path Across the Wide Plate

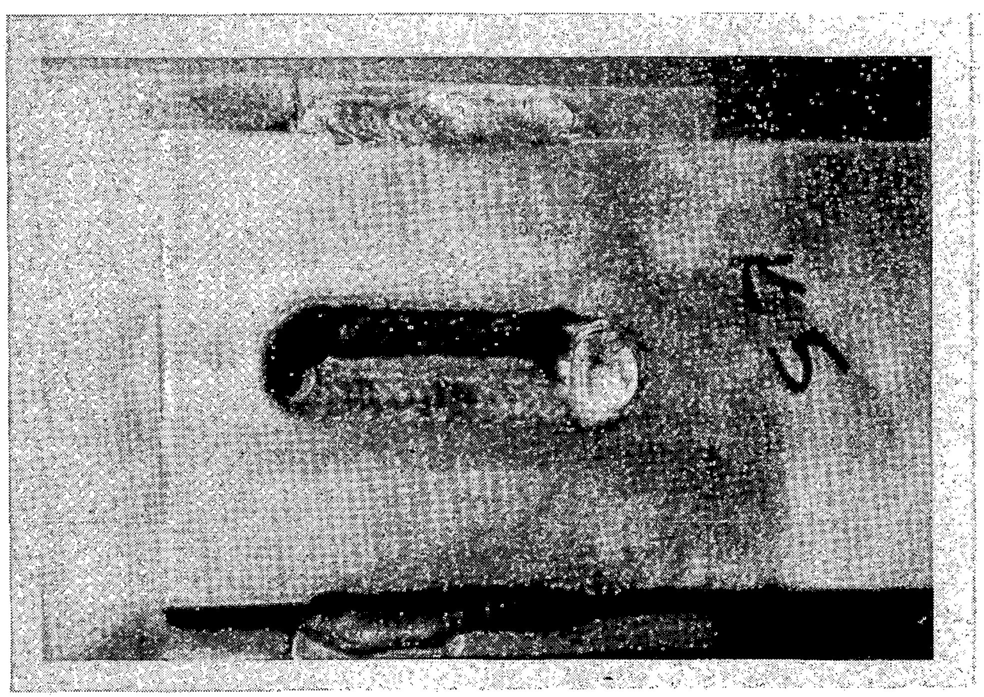

Fig. A20 Series K Showing Crack Extending Out From Slotted Plate

ASSOCIATION
OF AMERICAN
RAILROADS